Wireless Insufflation for Wireless Capsule Endoscopy

By

Byron Smith

Thesis

Submitted to the Faculty of the

Graduate School of Vanderbilt University

partial fullfillment of the requirements

for the degree of

Master of Science

in

Mechanical Engineering

December, 2012

Nashville, Tennessee

Approved:

Robert Webster III

Pietro Valdastri

Thomas Withrow

Acknowledgments

This work is the product of international, cross-disciplinary, and collaborative efforts. This work could not have been completed without the aid of supportive and inspiring flatmates, labmates, coworkers, friends and family. While brevity precludes me from thanking each and every contributor individually, I would like to specifically thank a few key collaborators.

I would like to thank Vanderbilt University for the financial support which made this work possible.

I would like to thank Robert Webster for providing me with the opportunity to pursue this work.

I would like to thank Pietro Valdastri for sharing his time, talent and toys with me.

I would like to thank Jonathon Rogers and Nicodemo for providing machining expertise.

I would like to thank Jason Gerding for suggesting the use of acid/base reactions in this work.

I would like to thank Jeff Paine and Patrick McGirt for the feedback and insight they so graciously shared with me throughout this project.

I would like to thank Keith Obstein for sharing his insights as a clinician and film director.

I would like to thank the committee members for their feedback and insight during the drafting of this document.

I would like to thank Rachel Shoaf, Julie Donahue and Harold and Maude Little for being excellent flatmates during the drafting of this document.

I would like to thank Myrtle Daniels, Jean Miller, Suzanne Weiss and Nilanjan Sarkar for their assistance, support and guidance in matters administrative, logistical and other.

Most of all, I would like to thank Jenna Gorlewicz, Sissi Battaglia, Gastone Cuiti, Christian Di Natali, Massimiliano Simi and Marco Beccani for their assistance during every stage of this project. Particular thanks goes out to all who assisted during stages involving tissue prep or use.

Abstract

Robotic mechanisms promise to enhance the diagnostic abilities of capsule endoscopes, endow them with novel interventional capabilities and reduce the invasiveness of endoscopy. The success of traditional endoscopy in diagnosing disease of the gastrointestinal (GI) tract can be attributed to the clear view that such techniques provide of the intestinal lumen and the range of motion they are capable of displaying. When viewed in the context of capsule endoscopy, the ability to clearly view tissue and navigate within the GI track both depend on the ability to distend tissue. In an effort to bring this functionality to wireless capsule endoscopy, the present investigation examines the feasibility of generating a significant volume of gas from a capsule based-platform. Success of the system is determined by its ability to provide a level of insufflation that is necessary to enhance visualization, and allow for magnetic locomotion, within the colon. As such, this research begins by quantifying the amount of gas that must be introduced to the colon to enhance visualization and magnetic locomotion. Once the desired level of insufflation is established, various chemical reactions are evaluated for use as a gas generator within capsule-based devices. Finally, prototypes are designed, fabricated and tested to demonstrate the feasibility of wireless capsule insufflation.

Contents

List of Figures

List of Tables

Chapter 1

Introduction

1.1 Motivation

Wireless capsule insufflation (WCI) is an enabling technology poised to greatly enhance a number of Wireless Capsule Endoscopy (WCE) functions. Research groups in industry and academia have demonstrated the feasibility of enhanced diagnostic and interventional WCE platforms. However, reports of such work often fail to acknowledge the need for, or potential benefits provided by, insufflation. The present work looks to prove the feasibility of WCI in an effort to help advance the field of WCE. While WCI holds the potential to greatly impact wireless locomotion, and hence allow for advancement of almost all aspects of WCE, this work focuses on its potential impact on Colorectal Cancer Screening (CRC).

The sections that follow outline the supporting role WCI will play in WCE as a whole, and CRC screening in particular. A review of the current state of the art, with respect to WCE and CRC screening, is presented. Preliminary efforts to assess the levels of insufflation necessary to enhance visualization and allow for active magnetic-based locomotion are documented. Two potential strategies for developing the necessary gas are demonstrated and concept feasibility is exhibited in an ex-vivo porcine model.

1.1.1 Role as an Enabling Technology for Wireless Capsule Endoscopy

While little has changed with semi-flexible endoscopes since they were first made possible by the introduction of glass fibers in 1957, [1] a great deal of effort has been but forth on the development of accessories for endoscopes. Through the use of the endoscope's accessory port, physicians can deploy spectroscopy-based diagnostic measures [2], deliver hemostasis-promoting therapies [3], take biopsies, or remove large volumes of tissue including precancourse polyops or advanced carcinomas. In an effort to advance the field of WCE, researchers throughout the world are working to develop many of these same capabilities on-board capsule-based platforms (for example, capsule-based spectroscopy [4], capsule-based delivery of clips for hemostasis [5] and capsule-based biopsy [6], [7]). And while many of these modalities have been proven feasible in a single-capsule or multi-capsule platform, their implementation often requires (or at least would benefit from) the ability to insufflate the intestine.

At a fundamental level, the ability to inflate the intestine makes an endoscopist's job much easier. Rather than navigate through, and operate within, the compliant folds of the large intestine, the ability to distend tissue through the use of a pressurized gas or liquid provides the endoscopist with an enhanced view the endoscope's surroundings and a greater ability to move within said surroundings. In an effort to provide this same ease of motion and enhanced visualization to WCE, the present investigation looks to develop a capsule-based platform that, when remotely activated,

can deliver a volume of gas sufficient for enhancing local visualization and freedom of movement.

While the technology presented in this work looks to improve many aspects of capsule endoscopy, its technological, societal and financial impact are likely to be most warmly received initially by the colorectal cancer screening community. To that end, the subsequent section outlines the motivational role which advancing colorectal cancer (CRC) screening technology plays in the development of this work.

1.1.2 Potential Impact on CRC Screening

Colorectal cancer (CRC) is a proven killer that affects one in five Americans [8]. In 2012 alone, CRC is expected to take the lives of 51,690 Americans [8]. The good news is findings from a long-term multi-institution study (The American Cancer Society, the Centers for Disease Control and Prevention (CDC), the National Cancer Institute (NCI) and the North American Association of Central Cancer Registries (NAACCR)) shows that the incidence of CRC has been on a steady decline for both men and women over the last two decades [9]. In an effort to uncover the reason for this trend Edward et al. [9] preformed rigorous statistical modeling and analysis of data spanning over three decades. While their data clearly shows a 30% decrease in CRC incidence over the period from 1985 to 2000, their statical modeling suggests approximately half of that decline can be attributed to increased screening and its allowing for early intervention, while the other half is the likely result of increased knowledge of the risk factors associated with CRC (e.g. smoking [10] , obesity [11], red meat consumption [12], low aspirin use [13], vitamin deficiencies [14] and physical

inactivity [10]).

The contributions that patient knowledge provided in reducing CRC incidence are certainly significant, however, the contributions provided by increased compliance with screening guidelines serve as a prime motivator behind many of the advancements in endoscopy that have been seen over the last decade. The American Cancer Society reports a 5-year survival rate for stage IV CRC of just 6% and a 74% survival rate for stage I diagnoses, when symptoms are often not apparent [15]. With numbers like these, and only roughly a third of Americans adhering to recommended CRC screening guidelines [9, 16], one can easily extrapolate the lack of compliance with suggested screening guidelines is a likely result of the invasive, and often painful, nature of current screening methods. This is an assumption that researchers are proving valid [17]. While devices like PillCam^{TM}COLON look to mitigate the deterrents to CRC screening by providing a minimally invasive method for imaging the interior lining of the colon, current capsule-based colonoscopy techniques suffer from low sensitivity in the detection of even advanced neoplasia [18]. Such results often occur when a lesion is hidden from the camera's view by folds in the intestinal tissue. During traditional colonoscopy, such lesion are brought into view by inflating the colon to unfurl folds. However, to date, capsule endoscopy lacks the ability to provide insufflation.

1.2 Current State of the Art: CRC Screening

Current protocols for CRC screening vary depending on age, risk factors and advising agency. As an example, The Center for Disease Control and Prevention (CDC) suggests men and women between the ages of 50-75 be screened using High-Sensitivity

Fecal Occult Blood Testing (FOBT) each year, flexible sigmoidoscopy every five years, or colonoscopy every ten years [19]. Alternatively, the American Society for Gastrointestinal Endoscopy suggests a preferred modality of colonoscopy every ten years, but also list alternatives consisting of yearly FOBT and sigmoidoscopy every five years [20]. Though opinions on screening guidelines may vary, there is wide consensus among physicians and researchers that traditional colonoscopy remains the gold standard for preforming CRC screenings. Endoscopy-based colonoscopy is often preferred by physicians, and its use supported in the literature, due to the versatile diagnostic and therapeutic capability. Despite the stellar reputation that colonoscopy-based CRC screening has earned, studies have shown that patients are half as likely to keep a scheduled CRC screening appointment if they know they are going to receive a traditional colonoscopy when compared to minimally invasive screenings like (FOBT) [17].

In recent years, the quest to develop less invasive screening methods has fueled advancements in FOBT, virtual colonoscopy (VC) and capsule-based endoscopy (CE). While the use of FOBT as a screening modality has received relatively widespread acceptance, VC remains a cutting-edge technology that is not often utilized and CE still seeks to prove its capacity to evaluate the colon. In what follows, the strengths and weakness of the above-mentioned screening methods are discussed.

1.2.1 Flexible Sigmoidoscopy

Flexible sigmoidoscopy is similar to colonoscopy but allows the physician to inspect up to the sigmoid colon whereas colonoscopy allows the physician to evaluate the entire colon. When compared with colonoscopy, sigmoidoscopy enjoys improved safety (rate of perforation of 4/25,000 vs 14/25,000) and a lower cost [21]. Like colonoscopy, flexible sigmoidoscopy is invasive; however, sedition is often not required. While a number of advisory organizations still list flexible sigmoidoscopy as an option for cancer screening, a growing number of physicians are acknowledging that its use as a CRC screening modality may be outdated [22].

1.2.2 Fecal occult-blood testing

Fecal occult-blood testing (FOBT) is a general term used to describe a range of diagnostic tools which are based on testing a patient's stool for the presence of blood. More specifically, the two main commercial FOBT technologies detect two different classes of hemoglobin products in feces. Guaiac FOBT (gFOBT) detects heme while fecal immunochemcial test (FIT) detects globin. Based on the underlying principles of gFOBT, this method of FOBT is not selective for bleeding originating in the colon and rectum alone. gFOBT is also prone to false-positives that can result from the consumption of certain fruits and vegetables, as well as aspirin. False-negative results have also been linked to antioxidants such as vitamin C [21]. Alternatively, FIT is not subject to interference from drug and dietary selection [23]. Since globin is rapidly digested in the stomach and small intestine, FIT is much more selective than gFOBT

when it comes to detecting occult bleeding of colorectal origin. Whether it be gFOBT or FIT, FOBT simply provides a method for identifying individuals that should be refereed for colonoscopy and of providing said individuals with compelling evidence for following through with colonoscopy [23].

1.2.3 Virtual Colonoscopy

While FOBT can provide physicians within an indication as to whether further investigation of a patient's GI tract is warranted, virtual colonoscopy provides the clinician with a method for visually inspecting the GI tract. This visual inspection is conducted using a virtual 3D representation generated from computerized tomography (CT) or magnetic resonance imaging (MRI) data. During a typical procedure, the patient begins by taking a colon preparation identical to that used during traditional colonoscopy. The patient is then placed in a CT or MRI system and their colon is inflated using approximately 3L of room air or carbon dioxide. The imaging system is then used to scan the patients abdomen in order to generate the 3D rendering of the colon.

In principle, VC offers the ability to inspect the colon in a non-invasive manner. In practice, VC requires the use of insufflation to provide clear images; hence, while VC offers the promise of non-invasive imaging of a patent's GI tract, the actual implementation of VC still requires the invasive introduction of an air line in order to provide insufflation. The use of insufflation has been found to result in perforation of the colon in a small percentage of patients ($< 1\%$) [24]. Furthermore, the use of CT or MRI data to construct a virtual rendering of a patient's GI tract renders this

technique relatively expensive when compared to alternative screening methods [25]. Also, the use of advanced imaging modalities often reveals extracolonic or incidental abnormalities which must then be investigated, further adding to the cost associated with using VC as a CRC screening modality.

1.2.4 Capsule Endoscopy

Similarly to VC, capsule endoscopy (CE) allows a physician to view the interior lining of a patient's colon. However, in the case of CE, the physician's view of the colon consists of thousands of still images taken from a camera embedded within a swallowable capsule. This imaging technique not only results in sharper image quality with respect to VC, it also holds promise for providing physicians with a real-time method for exploring the colon. Since WCE was first introduced by Given Imaging Inc. in 2000, more than one million capsules have been used by patients (per press releases from Given Imaging, Inc.). While this technology has certainly been well received by patients and physicians alike, commercially available capsule endoscopes currently only serve as passive observers as they travel through the GI tract while being propelled by peristalsis. A growing body of research is showing how these devices might one day allow physicians to precisely control the position and orientation of capsule endoscopes and even provide therapeutic capabilities.

Commercial entities including Given Imaging, Olympus and Philips have all made recent attempts to develop capsule-based methods for reliably preforming capsule-based colonoscopy. To date, their efforts have included methods for actively controlling the location and pose of the capsule and adding additional cameras to a capsule

to provide increased likelihood of capturing clinically-relevant images. Such efforts have resulted in a capsule (PillCam^{TM}COLON) that has sought FDA approval as a screening method for CRC; however, a recent report in the New England Journal of Medicine shows that PillCam^{TM}COLON suffers from a high false-negative rate [26]. One reason for the false-negative rate in PillCam^{TM}COLON has been attributed to its inability to visualize sites of interest that are obscured by folds in the colon lining [7]. Hence, a logical step in reducing false-negative rates may be the development of a wireless insufflation platform that could be used to enhance visualization in wireless capsule colonoscopy.

1.3 Thesis Contributions

A method of wireless insufflation for use in minimally invasive endoscopy: The following work provides an assessment of the feasibility of wireless capsule-based insufflation. Wireless insufflation looks to enhance wireless capsule endoscopy by enhancing visualization and, in the case of magnetic locomotion, enhancing mobility. In order to make a case of the feasibility of WCI, experiments are conducted to determine the amount of gas required to enhance visualization within the colon and allow for magnetic locomotion. The design of wireless insufflation capsules having dimensions on par with that of commercially available capsule are presented. Prototypes of said capsules are constructed and feasibility of wireless capsule insufflation is demonstrated in an ex-vivo model.

Chapter 2

Functional Requirements

This chapter establishes insufflation levels that are required for enhancing visualization of, and locomotion through, the colon during WCE. Experimental results are presented which look to quantify the amount of gas needed to enhance visualization and locomotion. This data is required to assess the feasibility of delivering a sufficient amount of gas from a given capsule with a given chemical reaction. This data is also needed to inform the design process described later in this thesis.

2.1 Need for Establishing Functional Requirements

One common challenge all endoscopic capsules must contend with is the distention of tissue away from the device, and particularly away from the face of the on-board camera (see Figure 2.1 (a)). This is especially important in the large intestine, where the intestinal lumen is much larger than the capsule diameter. Traditional endoscopes achieve distention by inflating the intestine with air. Such insufflation provides a much clearer view of the wall of the intestine, as can be seen in Figure 2.1 (b). It should be noted, however, that insufflation is not without drawbacks. Inflation can cause moderate to severe pain [27] and use of the wrong insufflating medium can result in disastrous and, at times explosive [19], consequences. While room air is commonly used as an insufflating medium, carbon dioxide [27, 28], helium [29] and water [30] have also been investigated as distending mediums.

In a 2004 study presented by Burling at el., researchers found that, when using an automated CO_2 delivery system with pressure-based closed-loop control during

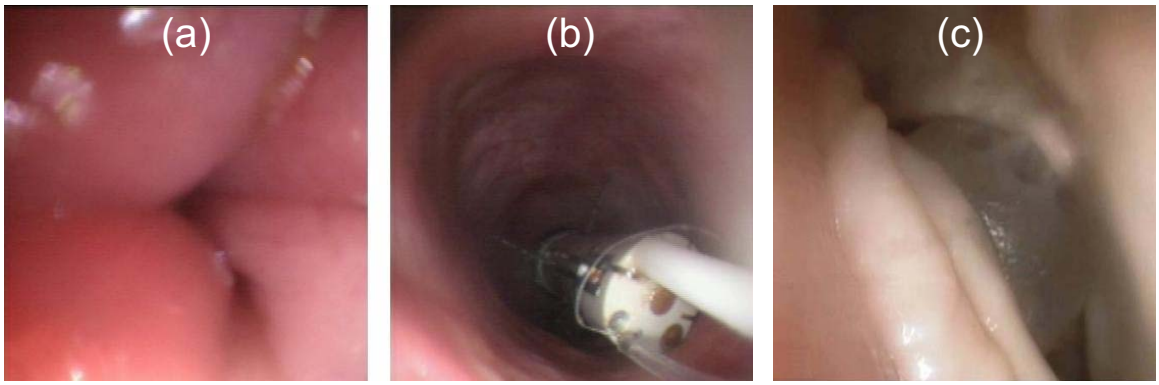

Figure 2.1: (a) An image from a colonoscope of the colon prior to insufflation. (b) An image after insufflation. Note that in this image much more of the intestinal surface can be seen. Also pictured here is a prototype of a capsule robot with legs [31].(c) An image showing a capsule controlled by external magnetic fields (e.g. [32]) that has difficulty moving through collapsed intestinal folds (as do other capsules with active locomotion) of an un-inflated colon.

VC (rectal pressure of $\leq$15mm Hg initiates insufflation while pressures $\geq$25mm Hg terminate the introduction of gas), automated delivery of 1.9L to 4.5L (median 3.0L) of CO_2 resulted in higher distention scores when compared to a control group which received 3.0L of manually administered CO_2 (3.20L (SD, 1.16L) and 3.22L (1.12L) for the supine and prone scanning positions, respectively, versus 2.86L (1.27L) and 3.00L (1.20L) for the case of manual insufflation) [33]. A statical analysis presented by Burling indicated that increased volumes of insufflation did not always result in increased distention scores, indicating that maximum distention and optimal distention are in fact not identical.

In the case of traditional colonoscopy, Bretthauer et al. found that, when instructing endoscopists to use as little insufflation as possible to achieve adequate visualization, physicians typically administered 8.3L of CO_2 (range 1.2-19.8 L) compared to 8.2L of air (range 1.8-18 L) with mean insufflation rates of 0.26 and 0.24

L/min, for the cases of CO_2 and room air, respectively. A similar study conducted by Leung et al. found an average of 1.3 ($\pm$0.593) L of water were required to provide adequate visualization during routine colonoscopy [30]. The difference between volumes reported by Burling, Bretthauer and Leung illustrate the vast disparity in experimental protocols and reporting conventions that currently exist in the literature.

With the average human large intestine measuring approximately 6cm in diameter and 1.5m is length, the total volume expected to fill a colon is on the order of 4.4L. With Burling at el. reporting that optimal distention is slightly less than maximum distension, their numbers regarding the volume of insufflating gas used during VC seem to be on par with what one might expect. Conversely, when one considers Bretthauer's et al. claim that upwards of 8L of CO_2 or room air might be administered during a traditional colonoscopy, the reported value may seem unreasonably high. A possible explanation for this discrepancy is that Bretthauer et al. were reporting the total volumes administered, and these values do not discount volumes of gas that are withdrawn during the course of the procedure. While studies reporting the volumes of insufflation used during VC may be less than half of that used during traditional colonsocpy, the use of pressure-regulating automated insufflation systems in VC can result in a higher incidence of overdistention when compared to traditional colonoscopy even though the latter has been reported to use twice the volume to achieve insufflation. Regardless of the cause of the discrepancy between reported volumes of insufflating gas, the occurrence of said discrepancies, and Burling's at el. observation that maximum distension is not always optimal distention, underline the

fact that different CRC screening modalities require different levels of insufflation.

While a number of studies have been presented in the literature regarding the volumes of carbon dioxide or room air that are typically needed during traditional colonoscopy [30] and VC [33], to date, little has been published on the volumes of gas required to enhance visualization and mobility in WCE [34, 35]. With reports concerning the volume of gas necessary in traditional and VC showing dependence on the type of medium used and the manner by which insufflation is administered, the present investigation looks to experimentally evaluate the volumes of gas necessary to enhance visualization and locomotion in WCE. In the sections that follow, experimental procedures are described which look to assess the levels of insuffllation necessary for enhancing visualization and mobility of wireless capsule endoscopes.

2.2 Enhancing Visualization

To determine the amount of fluid a capsule must carry in order to enhance visualization within the colon, an ex vivo experiment was performed using porcine large intestine. The experiment sought to quantify the effect insufflation has on enhancing visualization. Once relevant levels of insufflation were determined, these values can be used in conjunction with information concerning the expansion ratio produced by various chemical reactions to determine the amount of initial volume needed to produce a desired level of insufflation with a given chemical process.

In the present work, the porcine model was selected for its relative comparability to the human GI tract. The porcine model has been used to study a number of CRC screening modalities including active locomotion capsule endoscopy [36, 37], virtual

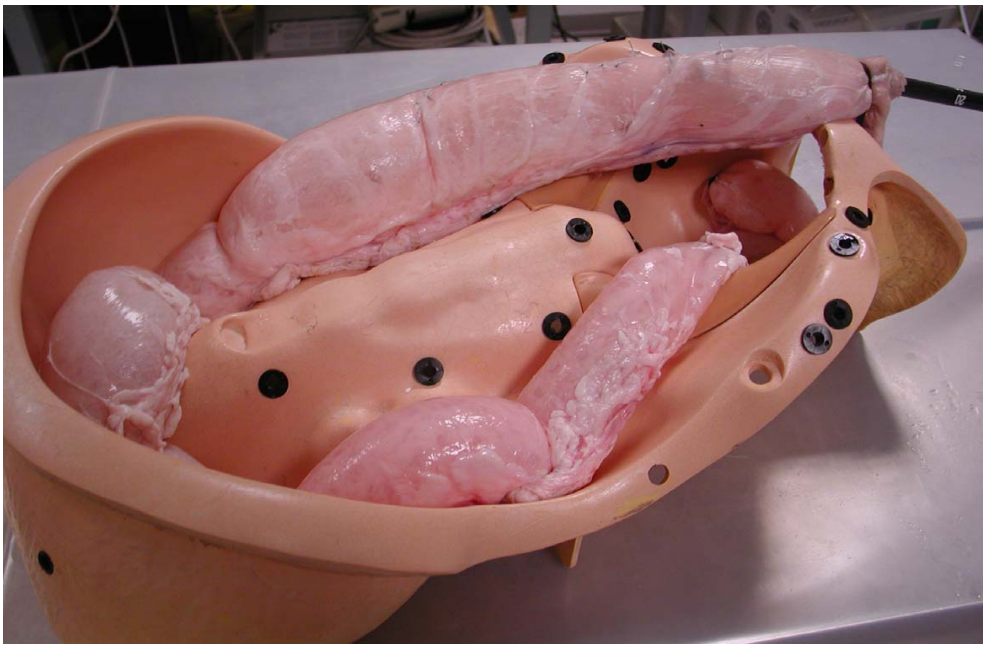

Figure 2.2: The experimental setup for a feasibility test conducted to determine how much insufflation is required to improve visualization within the large intestine. Ex vivo porcine intestine was arranged in a phantom model to simulate the shape of the human colon within the abdomen.

colonoscopy [38] and emerging endoscope platforms [32,39]. While the average length of a human adult colon (5 m) measures roughly a quarter of that found in an adult pig (18.5 m), when normalized with respect to weight, the anatomy of the human colon and porcine colon become quite comparable (average adult human mass is 80kg and average adult porcine mass is approximately 250kg). Therefore, in order to provide for an ex vivo trial that properly reproduces conditions similar to those found in the human colon, the porcine colon used in the following test were taken from pigs weighing 80-100kg. For a rigorous review of the similarities and difference between porcine and human anatomy, the interested reader is referred to [40].

The experiment used to determine the amount of insufflation necessary to enhance visualization consisted of placing nine colored markers inside a section of intestine

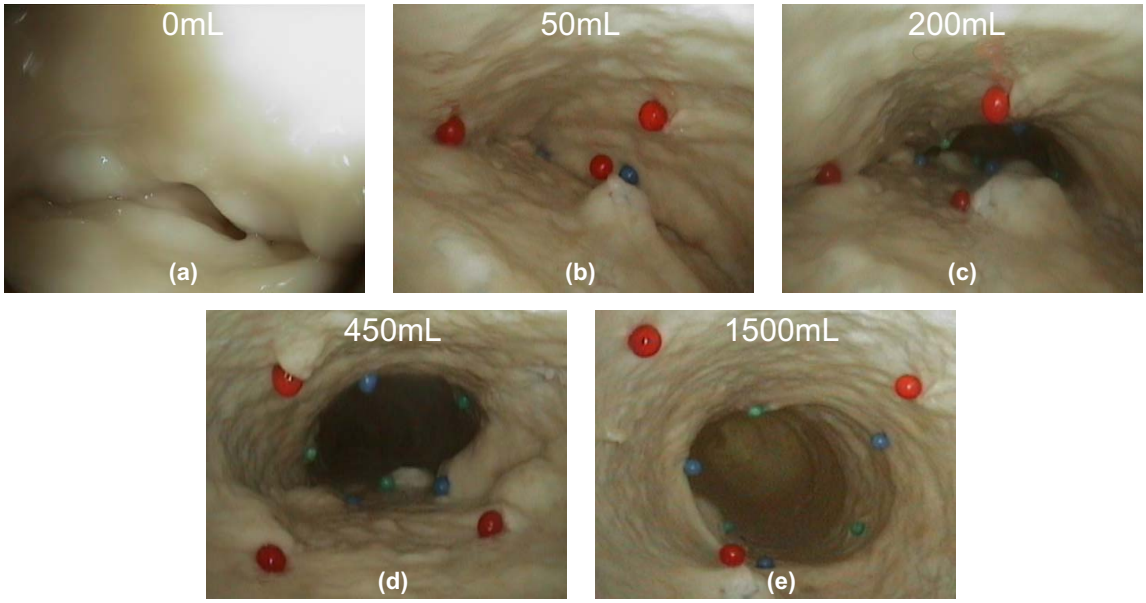

Figure 2.3: The results of the first feasibility test at different inflation increments. (a) The intestine in its deflated state with no markers visible. (b) With just 50mL of insufflation, 4 of the 9 markers became visible. (c) At 200mL, all 9 markers first come into the field of view. (d) The threshold above which all 9 markers were consistently visible was 450mL. (e) The intestine in its fully inflated state at 1500mL of insufflation.

measuring 150 cm by 6 cm in diameter. The fiducials were evenly spaced throughout the large intestine with 3 markers placed around the inside diameter of the intestine and this pattern being repeated twice along the length of the intestine with approximately 3cm between groups of markers (see Figure 2.3). The deflated colon was then placed inside an anatomical model of the human torso, as shown in Figure 2.2. A flexible endoscope (13803PKS endoscope, Karl Storz GmbH & Co. KG) was then placed approximately 4 cm from the first set of markers in an effort to visualize the fidicuals in a manner similar to that which might be achieved using a capsule robot. A controlled air compressor was used to locally insufflate the intestine from the initially deflated state to a state where all nine markers were consistently visible by incrementing the level of insufflation 50mL at a time. An in-line flow sensor (AWM3300V,

Honeywell) was used to determine the volume of gas introduced into the intestine.

During the experiment, images were obtained at each volume increment immediately after the level of inflation was incremented and 30 seconds later in order to assess time-dependent effects. While appreciable time dependent behavior was not observed, it was interesting to note the manner by which insufflation occurred. Rather than gradually inflating the entire colon in a uniform manner, a small section surrounding the introduction site inflatted first and then this inflation bubble grew along the length of the colon as additional air was introduced. Table 2.1 shows the number of markers that were visible at various levels of insufflation. As can be seen from the chart, all nine markers were found to be consistently visible when 450mL of gas or more were used to insufflate the sample.

Table 2.1: The number of markers visible (out of 9 total) for each inflation volume. Above 450mL, all 9 markers were consistently visible.

Air Volume (mL)	Markers Visible
0	0
50	4
100	5
150	8
200	9
250	8
300	7
350	9
400	7
450	9
1500	9

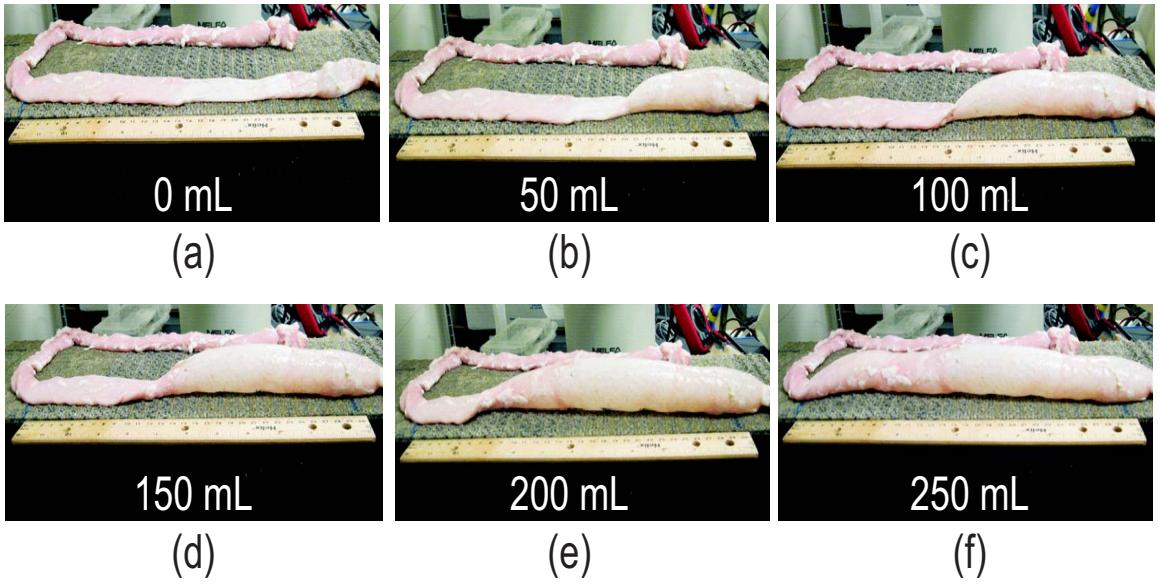

Figure 2.4: Photos of locomotion experiment at different inflation increments. (a) The intestine in its deflated state, where no capsule motion was possible. (b) With just 50mL of insufflation, the capsule moved an average distance of 66.7mm. (c) At 100mL,the capsule moved an average distance of 150mm. (d)At 150mL, the capsule moved an average distance of 188.3mm. (e) At 200mL, the capsule moved an average distance of 243.3mm. (f) At 250mL, the capsule was able to move the entire length of the colon (300mm), with an average distance of 295mm.

2.3 Enhancing Locomotion

Wireless insufflation offers the possibility to enhance visualization for passively locomoted capsule endoscopes and actively locomoted capsules alike. However, in the latter group, wireless insufflation may actually be necessary for the platform to function at all. Due to the complaint nature of the GI lumen, active locomotion techniques like magnetic guidance often have difficulty traversing the entire length of the lumen [35]. In order to assess the benefit wireless insufflation might have on magnetically-actuated capsules, a second insufflation experiment was conducted using porcine large intestine, a magnetic capsule, an external magnet and robotic arm.

In this second experiment a 1.21T NdFeB N35 permanent magnet (Sintered NdFeB

magnets, B and W Technology and Trade GmbH, China) with a diameter of 60mm, a length of 70mm and a weight of 1.5kg, was attached to the end effector of a 6 degree of freedom Mitsubishi RV-3S serial manipulator (Mitsubishi Electric Inc.). Three smaller internal magnets, (MTG Europe Magnet Technology Group, Germany), each having a diameter of 3mm, a length of 10mm, and a magnetic flux density of 1.21T, were placed inside of a pill-sized capsule (11mm diameter by 26 mm long). The working distance between the internal and external magnets was 150mm [32]. The robotic arm was preprogrammed to follow a straight path trajectory using Cosirop 2.0, a Mitsubishi Electric programming platform that allows simple functions to be written in a Basic-like language (Melfa Basic IV) and uploaded to the robotic controller by TCP/IP communication. The trajectory was 300mm long, which approximates the length of the longest straight portion of the colon. The robot would stop its motion every 10mm, rotate around its Z axis (roll angle) by 10 degrees, rotate around its Y axis (yaw angle) by 10 degrees, and then continue forward motion at a velocity of 5mm/s. The rotational speed was between 5 and 10 degrees/s. This behavior was performed in order to attempt to free the capsule from the deflated lumen as a surgeon might try through teleoperation.

The magnetic capsule was placed inside fresh porcine large intestine (4mm diameter), and the intestine was sealed at both ends. A 50mL syringe was connected to a tube whose outlet was located right behind the capsule and was used to incrementally inflate the intestine in 25mL intervals from 0mL-250mL. As shown in Figure 2.4, this resulted in local inflation of the colon, such that the capsule could advance up until the inflation bubble ended. Three trials were performed at each insufflation interval.

Results from this set of experiments are presented in Figure 2.5.

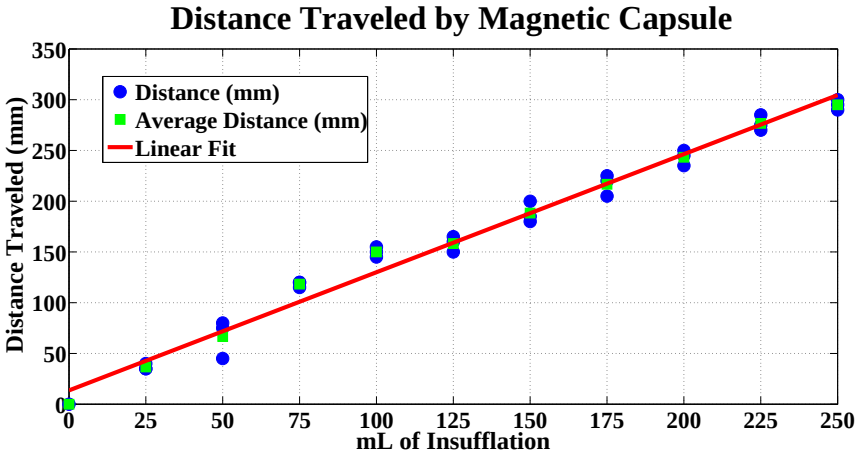

Figure 2.5: The distance the capsule traveled (mm) at each inflation increment.

Chapter 3

Chemical Reactions for Insufflation

This chapter presents various reactions that may be used for gas generation in wireless insufflation. Quantitative assements are made to determine the relative volume each reaction might produce when initial volumes of the reactants are kept on par with the volume of commercially available capsule endoscopes. Experimental findings are used as a guide in the subsequent development of WCI prototypes in later chapters.

3.1 H_2O_2 Decomposition

Using the gas volumes reported in Chapter 2, we now determine the necessary fluid volume required to produce each. Hydrogen Peroxide is a promising working fluid because it can produce a large volume of gas from a small initial fluid volume. To generate gas from H_2O_2, the capsule must simply pass liquid H_2O_2 through a catalyst (e.g. a silver or platinum screen), which catalyzes the conversion to oxygen gas and water.

In order to investigate the effect H_2O_2 concentration has on the amount of gas generated by this exothermic process, known quanities of 30%, 50% and 70% solution were reacted and the amount of gas generated was recorded. The experimental setup, shown in Figure 3.1, involved a mixing flask, a holding flask, and a discharge cylinder. The flasks were connected together with rubber tubing and were sealed with rubber stoppers. A thermocouple was used to measure the maximum temperature of the reaction. The catalyst used was a fine silver screen mesh, and it was cut into 11mm circles to replicate the maximum sized screen that could fit within a swallowable

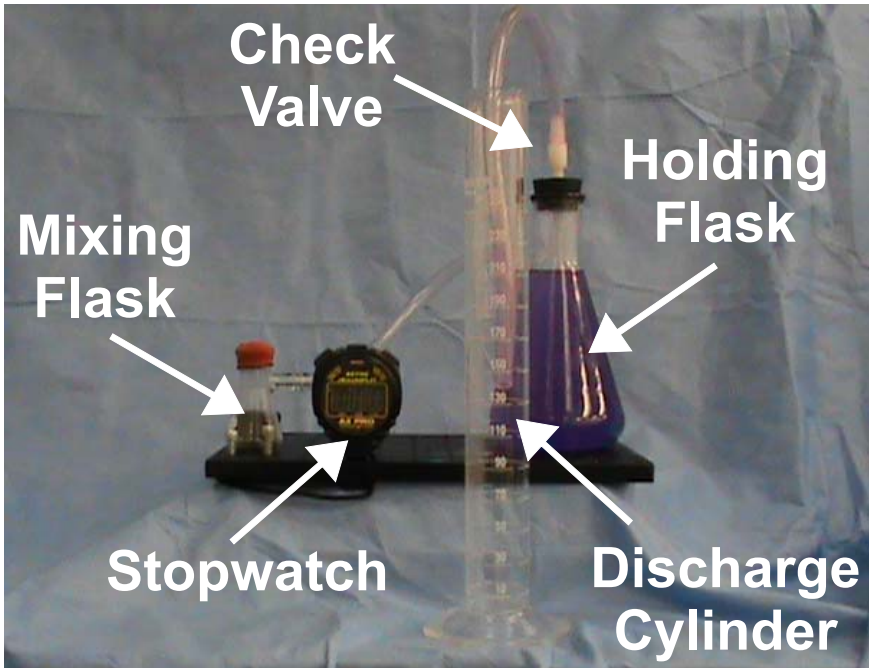

Figure 3.1: Experimental setup for reacting known volumes of H_2O_2 to measure gas production. A silver screen catalyst was dropped into the mixing flask which held a small initial volume of H_2O_2. The gas generated displaced water in the holding flask which was measured in a graduated cylinder.

capsule. An initial amount of Hydrogen Peroxide was placed in the mixing flask. The catalyst was quickly dropped into the flask, and the flask was sealed. The gas produced from this reaction was transferred to the holding flask, which held water that was displaced up a plastic tube, through a check valve, and into a graduated cylinder. The amount of water displaced corresponded with the approximate amount of gas produced from the reaction. This test was performed with initial volumes ranging from 0.5-1.25mL (in 0.25mL increments) for three concentrations of H_2O_2 (30%, 50%, and 70%). Initial volumes of H_2O_2 were measured using a graduated syringe with graduations of 0.01mL.

To ensure repeatability, three trials were performed for each initial volume level. One catalyst screen was used for each increment (i.e., one screen was used 3 times

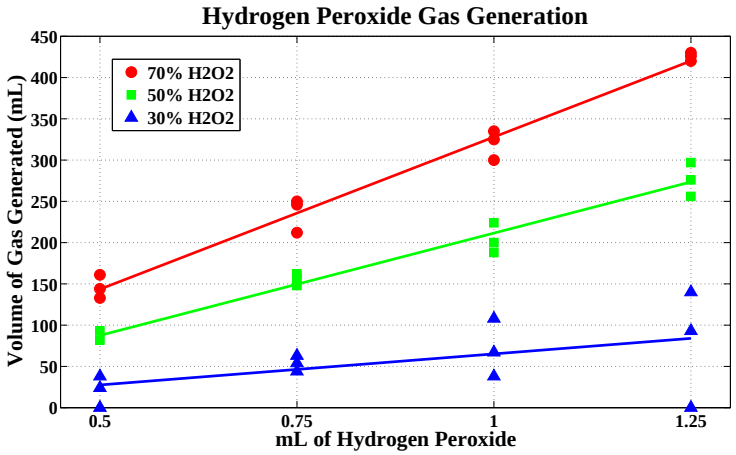

Figure 3.2: The volume of gas produced (mL) for initial amounts of liquid H_2O_2 at 30%, 50%, and 70% concentrations by mass.

at 0.5mL, and a new screen was used 3 times at 0.75mL). The amount of water output was recorded and averaged over the three samples for each increment, at each concentration, and the results are shown in Figure 3.2. The temperature on the bottom of the holding flask was measured to provide an assessment of the heat generated during decomposition and the maximum values recorded during each run are presented in Figure 3.3.

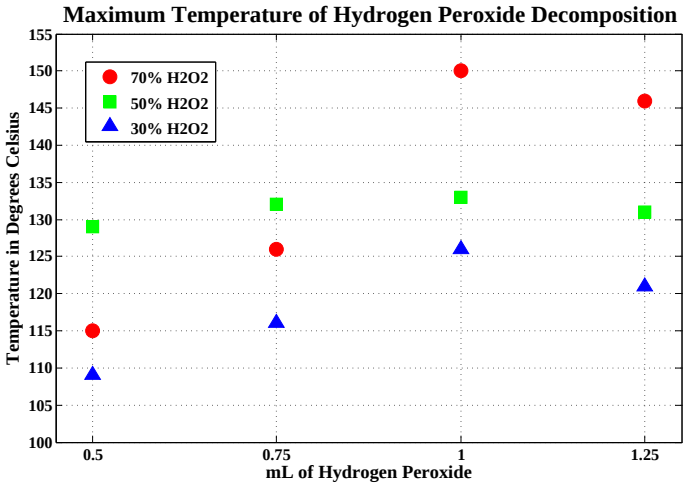

Figure 3.3: The maximum temperature recorded directly underneath the catalyst screen during the decomposition reaction. These temperatures were usually reached within seconds of the H_2O_2/catalyst interaction and were maintained during the time required for the H_2O_2 to decompose.

Table 3.1: Onboard capsule fluid volumes required to produce corresponding gas volumes from Chapter 2. The typical volume of a commercial camera pill is 2.47mL.

Gas (mL)	H_2O_2 70% (mL)	H_2O_2 50% (mL)	H_2O_2 30% (mL)
50	0.2571	0.3488	0.7103
100	0.3910	0.5504	1.167
150	0.5248	0.7520	1.6233
200	0.6586	0.9536	2.0798
250	0.7925	1.1552	2.5363
300	0.9263	1.3569	2.9928
350	1.0601	1.5585	3.4492
400	1.1940	1.7601	3.9058
450	1.3278	1.9617	4.3623
1500	4.1383	6.1956	13.9487

3.2 Acid/Base Reactions

Mild acid/base reactions offer a promising method for generating relatively large volumes of gas using small initial volumes of reactants. In order to generate gas using an acid/base reaction, the reactants need only be mixed in the presence of water so as to allow their constitutive anions and cations to disassociate. While the initial volume of the reactants directly affects the total gas generated by a given acid/base reaction, the rate of reaction is restricted by the anions/cations, ability to disassociate. Hence, the rate of reaction is dependent on the volume of H_2O present when the reaction takes place.

Given the desire to generate a relatively large volume of gas in a relatively short period of time, the total volume of initial reactants must be taken into account as well as ratio of reactant to H_2O volumes. In order to investigate the use of acid/base reactions as a gas generator for wireless capsule insufflation various acid/base combinations are theoretically and experimentally evaluated. Results from these investigations are used to select a promising acid/base combination. The use of this combination is then optimized by examining the effect that the initial reactant-to-H_2O ratio has on rate of reaction and total output produced, in a given time period.

In the present investigation acetic acid, citric acid, sodium bicarbonate and potassium bicarbonate are examined as possible reactants in an acid/base gas generator. These reactants give rise to four possible acid/base combinations, as is shown in Table 3.2. Given a desired total initial volume, the mass of the reactants, and the resulting output, can be calculated based on the physical properties of the reactants, as is

Table 3.2: Acid/Base Combinations. Clockwise, from upper left corner: A1B1 = Acetic Acid and Sodium Bicarbonate, A2B1 = Citric Acid and Sodium Bicarbonate, A2B2 = Citric Acid and Potassium Bicarbonate and A1B2 = Acetic Acid and Potassium Bicarbonate.

Bases \ Acids	A1	A2
B1	$C_2H_4O_2$ / $NaHCO_3$ (1)	$C_6H_8O_7$ / $NaHCO_3$ (2)
B2	$C_2H_4O_2$ / $KHCO_3$ (3)	$C_6H_8O_7$ / $KHCO_3$ (4)

outlined in Appendix B.

Figure 3.4 shows the output produced within the first fifteen minutes when an initial volume of reactants equal to 1.0mL is reacted in the presence of 0.5mL of H_2O. As can be seen in Figure 3.5, experimental results indicate that the combination of citric acid and potassium bicarbonate results not only in the largest average output but also the fastest rate of reaction. Figure 3.5 also shows that while citric acid and sodium bicarbonate offer the second largest average output, acetic acid and potassium bicarbonate offer the second fastest rate of reaction.

Based on the results presented in Figures 3.4 and 3.5 the use of citric acid and potassium bicarbonate offers the largest average output and fastest rate of reaction when constraints are placed on total initial volume of the reactants. In order to determine the effect that initial water volume has on rate of reaction and total output generated by this acid/base combination, additional experiments were preformed with initial water to reactant volumetric ratios of .25/1.25 and .75/.75 mL per mL. Results

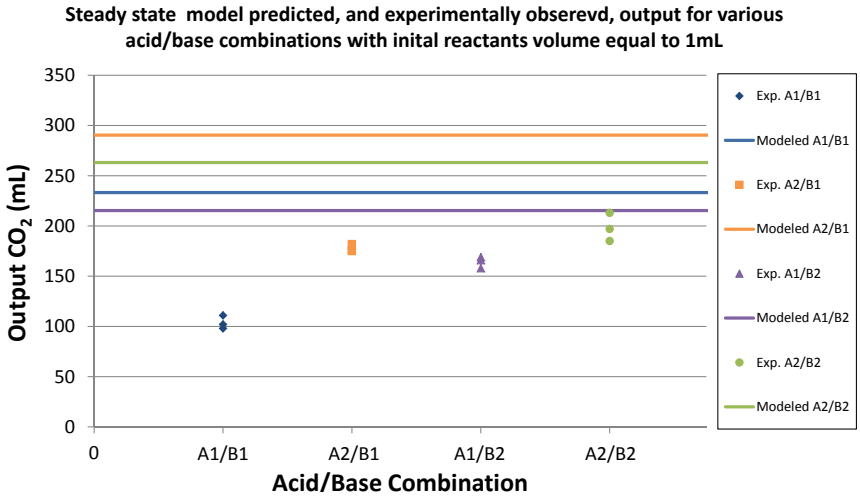

Figure 3.4: Theoretical predictions and experimental observations for the output produced by given acid/base combinations within the first fifteen minutes when an initial volume of reactants equal to 1.0mL is reacted in the presence of 0.5mL of H_2O.

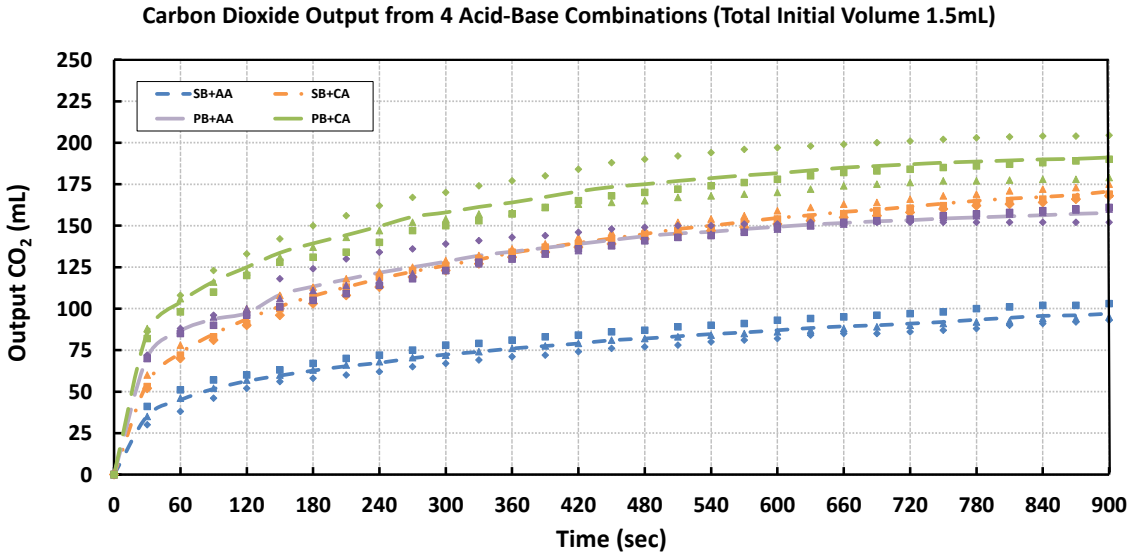

Figure 3.5: Transient output generated by various acid/base combinations when initial volumes of the reactants are set equal to 1.5mL.

from these test are presented, along with the case corresponding to an initial water to reactant volumetric ratio of 0.5/1, in Figure 3.6.

The results presented in Figure 3.6 indicate that while the relative volume of water present at the start of the reaction has an effect on the total output produced

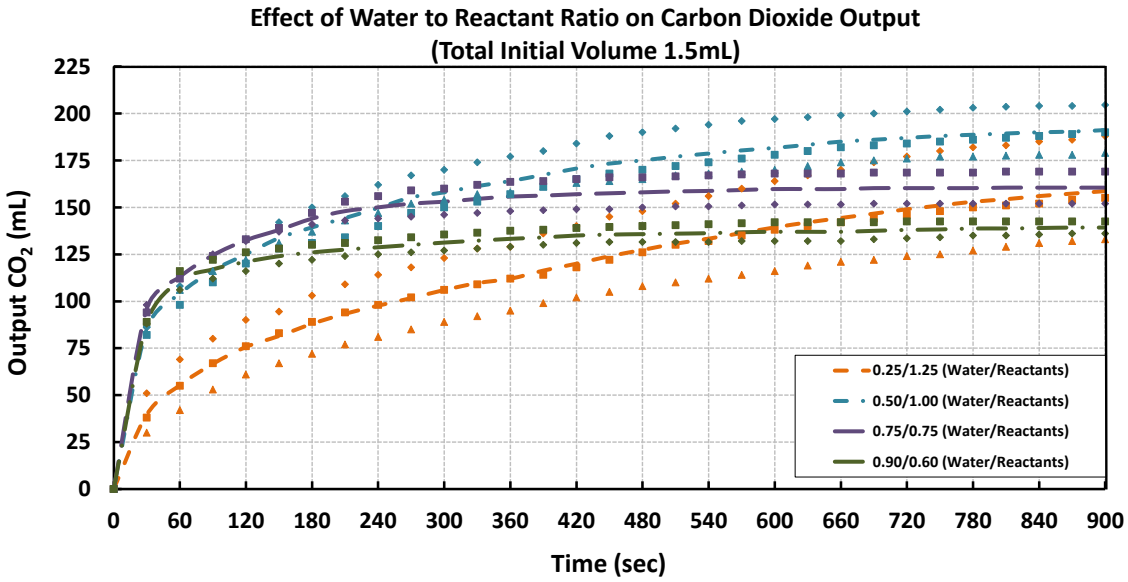

Figure 3.6: Transient output generated by citric acid and potassium bicarbonate when initial volumes of the reactants are set equal to 1.5mL and the volumetric water-to-reactant ratio is varied from 0.2 to 1.5.

from an initial quantity of reactants (i.e. more water in a given initial volume means less reactants and hence less output) they also illustrate the pronounced effect this variable has on the initial rate of reaction (i.e. the amount of output produced during the first moments of the reaction). With an average colonoscopy taking between 30 minutes to an hour to complete [41], a wireless insufflation capsule should be capable of generating the necessary volume of gas within some fraction of this time in order to keep WCE-based colonoscopy times on par with those conducted using traditional endoscopy. Based on the results presented in Figure 3.6 it appears as though, for a given total initial volume, a tradeoff exist between the amount of output that can be generated in a given time and total output that might be expected as $t \to \infty$. As can be seen from the data presented in Figure 3.6, a water-to-reactant volume ratio of approximately one-half-to-one seems to offer the best compromise between

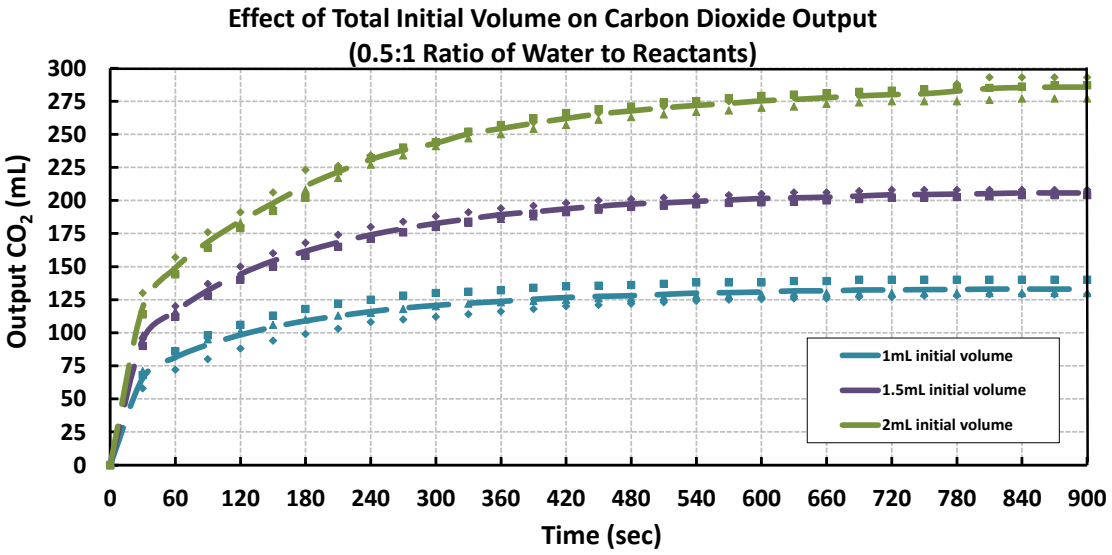

Figure 3.7: Transient output generated by citric acid and potassium bicarbonate when initial volumes of the reactants and water are set equal and total initial volumes are 1, 1.5 and 2mL

fast rate of reaction and total volume produced. If we redefine the examined water-to-reactant volume ratios in terms of initial grams of citric acid per initial volume of H_2O, the data presented in Figure 3.6 is classified by dilution as 3.78, 1.51, 0.75 and 0.50 grams of citric acid per milliliter of H_2O. It is interesting to note the case corresponding to an initial water-to-reactant volume of 1-to-1 provides a level of dilution that approximately matches reported values for the solubility of citric acid [42].

Using the information provided in Figure 3.6, a final set of experiments was conducted to determine the output generated when total initial volume is set equal to 1.0, 1.5 and 2.0mL and the water-to-reactant ratio is selected based on the results presented in Figure 3.6. These initial volume levels were selected based on the typical size of commercially available capsule endoscopes (2.47mL) and the likely usable volume within a capsule of said dimension. The transient output produced from said

initial volumes are presented in Figure 3.7. The linear trend presented in Figure 3.7 was extrapolated to determine the initial volume of reactants needed to produce desired volumes of CO_2. Results of said extrapolation are presented in Table 3.3. Based on the trend depicted in Figure 3.7, one might reasonably expect to obtain 450mL from a capsule containing powdered acid and base reactants or 300mL from a capsule containing reactants plus H_2O such that the initial water-to-reactant volume ratio is approximately one-half-to-one.

Table 3.3: Onboard capsule reactant and reactant plus water volumes required to produce corresponding gas volumes from the insufflation experiment. The typical volume of a commercial camera pill is 2.47mL.

CO_2 (mL)	$C_6H_8O_7 + KHCO_3$ (mL)	$C_6H_8O_7 + KHCO_3 + H_2O$ (mL)
50	0.22	0.33
100	0.45	0.67
150	0.67	1.00
200	0.89	1.34
250	1.11	1.67
300	1.33	2.00
350	1.56	2.34
400	1.78	2.67
450	2.00	3.00
1500	6.68	10.02

Chapter 4

Wireless Insufflation Capsule Design

This section introduces capsule designs which were developed to demonstrate the feasibility of wireless capsule insufflation. Preliminary efforts investigated the catalytic decomposition of hydrogen peroxide in addition to a number of effervescent reactions for use as possible gas generators in a WCI platform. While hydrogen peroxide was found to have an excellent expansion ratio, recent findings published in the Journal of Clinical Gastroenterology and Hepatology [43] have shown that even concentrations on par with the weakest solutions presented in Chapter 2 can result in serious damage when ingested. As such, the remainder of this work focuses on the use of effervescent reactions for the realization of WCI. Specifically, the designs presented in this chapter utilize citric acid ($C_5H_8O_7$) and potassium bicarbonate ($KHCO_3$) to generate carbon dioxide (CO_2). Based on the findings presented in Sections 2.2 and 2.3 we know that one or more capsules should be capable of providing approximately 450mL to locally enhance visualization, or, as little as 250mL to enhance locomotion in a section of colon approximating the length of the longest straight portion of the human colon.

4.1 Acid-Base Prototype Design

Based on the specifications for relevant volumes of gas needed to enhance visualization and locomotion within the colon, as presented in Chapter 3, two capsule architectures are proposed. In the first concept, the capsule will carry a payload comprised only of powdered reactants. When activated, said capsule will break apart, exposing its contents to the fluid found in the colon. This concept allows the capsule to maximize

achievable output by mitigating the need to carry H_2O. In the second concept, the capsule will carry one reactant in powdered form while the other will be diluted and carried as a solution. This design will allow for the reaction to be contained within the capsule. Throughout the remainder of this document, these two architectures will be referred as External Reaction Capsules (ERC) and Internal Reaction Capsules (IRC), respectively. The sections that follow present both capsule architectures in greater detail. While the ERC has the obvious advantage of being able to transport a larger volume of reactants for a given capsule volume, since it does not require that H_2O be carried onbaord, it does not provide the means to start and stop gas production. Conversely, while the IRC must forfeit some internal volume to the transportation of H_2O, carrying one reactant in solution form allows metered, or throttled, control over the rate at which reactants are mixed. Hence, the latter design sacrifices some output in order to provide control over when output can be provided. The functionality of initial prototypes is demonstrated in benchtop and ex vivo models.

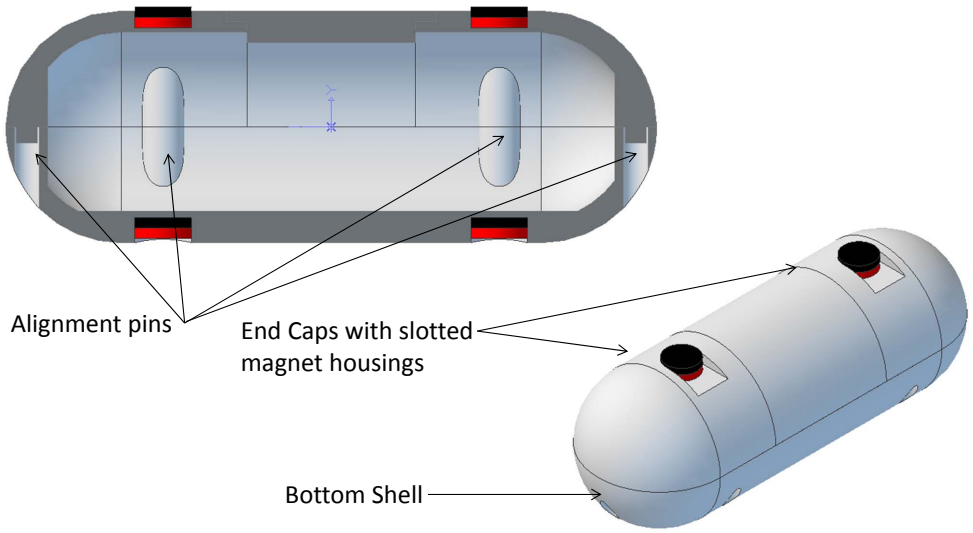

Figure 4.1: CAD rendering of the External Reaction Capsule showing internal alignment features, external closing magnets and slotted magnet housings.

4.2 External Capsule Design

One elegant design of a capsule which can be remotely triggered to allow for localized drug delivery has been recently introduced by Matesy GmbH. Their Magnetic Active Agent Release System, or MAARS, is comprised of a weakly magnetized ferromagnetic capsule, a 3D tracking system (3D-MAGMA) and an external magnetic field source. The MAARS system uses a 3D tracker to localize the capsule within the GI tract and when the capsule reaches the desired delivery site, the magnetic field source is used to demagnetize the constitutive pieces of the capsule such that they are no longer held together by magnetic attraction [44].

The MAARS concept looks to maximize the payload a capsule can carry by using a ferromagnetic shell in lieu of permanent magnets paired with more conventional

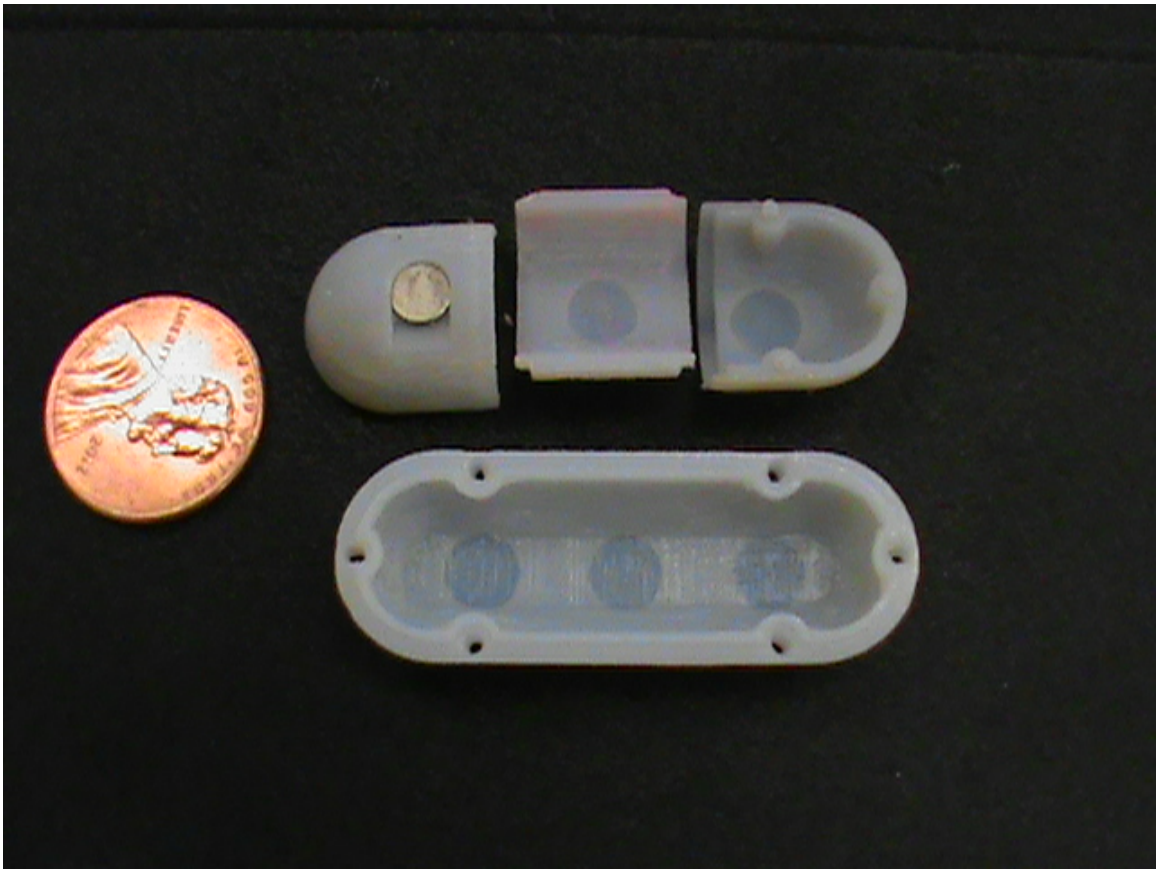

Figure 4.2: Various components of the first generation external reaction capsule showing slotted magnet housing

materials. In the present work, a MAARS-like capsule is constructed using a rapid prototyped shell (Objet30 Pro, Objet Geometries Inc. Billerica, MA) and four cylindrical permanent magnets. A CAD drawing of the External Reaction Capsule is presented in Figure 4.1. The capsule consists of a four piece shell, with three pieces defining the upper half and one piece defining the lower half. The lower half of the capsule contains female alignment features that mate with features on the two end caps. The end caps have additional mating features that align and constrain the upper center section of the capsule. An extrude cut on each end cap serves to locate a permanent magnet. Complimentary features on the lower chamber of the capsule are

also used to locate permanent magnets. When properly oriented and placed in said locating features, these two sets of magnets form a magnetic link between the upper and lower components. The capsule can be activated by introducing an external magnetic field strong enough to overcome the force generated by the magnetic couple that exists between the capsule's on-board magnets. Once said magnetic couple is overcome, moisture is free to enter the capsule and the reaction between the acid and base stored on-board begins. The onset of the reaction generates pressure which serves to further open the capsule, thereby allowing the contents of the capsule to become exposed to water found in the colon.

4.2.1 External Reaction Capsule: Ex-vivo Trials

Ex vivo trials were performed to obtain qualitative results from the reaction between potassium bicarbonate and citric acid. As was referred to in Section 3.2, this reaction resulted in the best solution in terms of yield of gas within the considered time interval, from the bench tests discussed in Chapter 3. The aim of these trials is the qualitative evaluation of colon lining visualization, as a measure of the accomplishment of the insufflation. Said evaluation was carried out using the experimental setup shown in Figure 4.3, which consisted of a heated bath, fiber-optic endoscope, image acquisition system, and a magnetic field source for actuating the capsules.

The experiment was carried out by immersing a porcine colon in a heated bath filled with 37^{o}C water. The colon, measuring approximately 4cm in diameter, was sutured to an acrylic sheet to maintain its position and orientation underwater. This was done in order to more accurately recreate the conditions found inside a human

Figure 4.3: Experimental setup used during ex vivo assessment of the ERC and the IRC.

colon with respect to temperature and pressure. A pattern of nine markers serving as fiducials, consisting of three rings of three markers each, was evenly spaced and sutured throughout the lining of the colon. The fiducials were evenly spaced throughout the large intestine with three markers placed around the inside diameter of the intestine and this pattern being repeated twice along the length of the intestine with approximately three centimeters between groups of markers, matching the layout and placement discussed in Section 2.2. The ERC was used to carry 2mL of powdered reactants to a location approximately 4cm past the deepest ring of markers. When the desired location was reached, the capsule was opened using the attractive force generated by an external magnetic field provided by a cylindrical magnet measuring

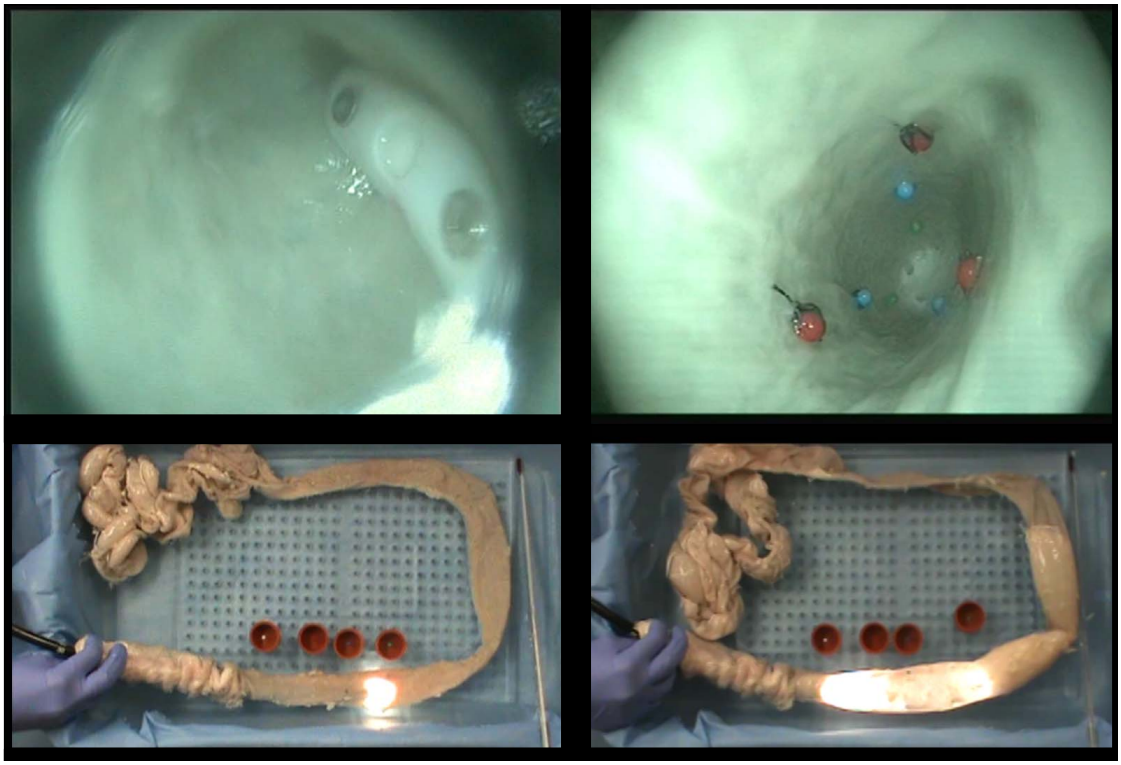

Figure 4.4: Internal (above) and external (below) views of the colon prior to (left) and following (right) activation of the capsule.

2" in length and 2" in diameter (K&J Magnetics, Product Number:DYOYO). Upon activation, the powdered chemicals react with water within the colon to produce the CO_2 responsible for insufflation. Three trials of this experiment were performed by an expert endoscopist who had previously performed more than 2,000 human clinical endoscopy procedures.

The images presented in Figure 4.4 show that the capsule was able to insufflate the section of colon to a point where most of the markers became visible. The picture presented in the upper right of Figure 4.4 shows eight of the nine markers. Based on the results presented in Section 2.2, this level of visibility corresponded to roughly 350mL of gas. While not all of the markers became visible during any one frame captured by the endoscope, based on our experience with magnetic locomotion in

section 2.3, the level of inflation is qualitatively similar to a level that would have enabled magnetic locomotion throughout the inflated part of the colon.

During the tests, a relatively large volume of foam was generated in the colon. The formation of foam is a natural byproduct of effervescent reactions. However, it was interesting to note that during different runs the size of air bubbles within the foam appeared to vary, as did the time required for said bubble to dissipate. Figure 4.5 shows foam escaping from the ERC and obscuring the view of the colon wall. While the ERC is not visible, the image shown in the upper right of Figure 4.4 also shows the formation of foam following activation of the capsule. With the majority of foam staying in close proximity to the capsule, it may be possible to activate one or more capsules at sufficient distance from the colon so as to allow insufflation while retaining foam in the small intestine. Alternatively, in the sections that follow, an Internal Reaction Capsule is presented that looks to mitigate the affect foam production has on visualization by retaining foam within a reaction chamber on-board the capsule.

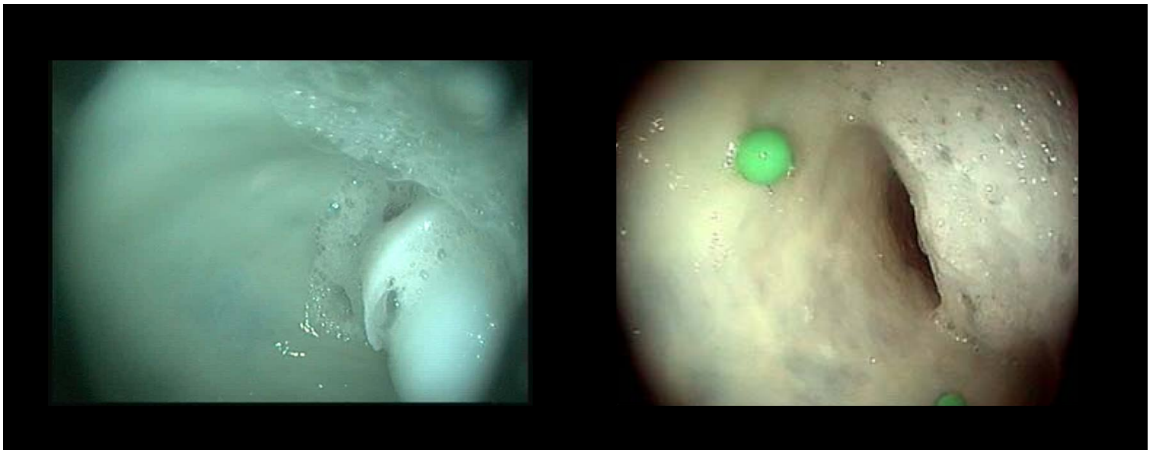

Figure 4.5: (left) Foam escaping the capsule and (right) obstructing the view of the colon wall.

4.3 Internal Reaction Capsule

4.3.1 Internal Reaction Capsule: Version One

The initial prototype for the Internal Reaction Capsule (IRC) consists of rapid prototyped capsule measuring 12mm OD, 10mm ID and, 32mm in length with a 1mm thick center divider that separates the upper and lower chambers (see Figures 4.6 and 4.7). The upper chamber of the capsule houses approximately 1mL of citric acid solution while the lower chamber is designed to hold approximately 0.64mL of base. The magnetic ball valve uses a grade N42, 1/8" diameter, magnetic sphere (K&J Magnetics, Inc. Model number S2). The attractive force used to keep the valve closed is provided by magnetic coupling with a steel ring (4.173 mm OD, 1.27mm ID, 0.1mm thick) which is mounted on the opposite side of the capsule's center divider. The capsule is activated by introducing an external magnetic field strong enough to unseat the magnetic sphere. Since the sphere is free to rotate in the valve seat an external field need only be a targeted distance from the capsule to open the valve as

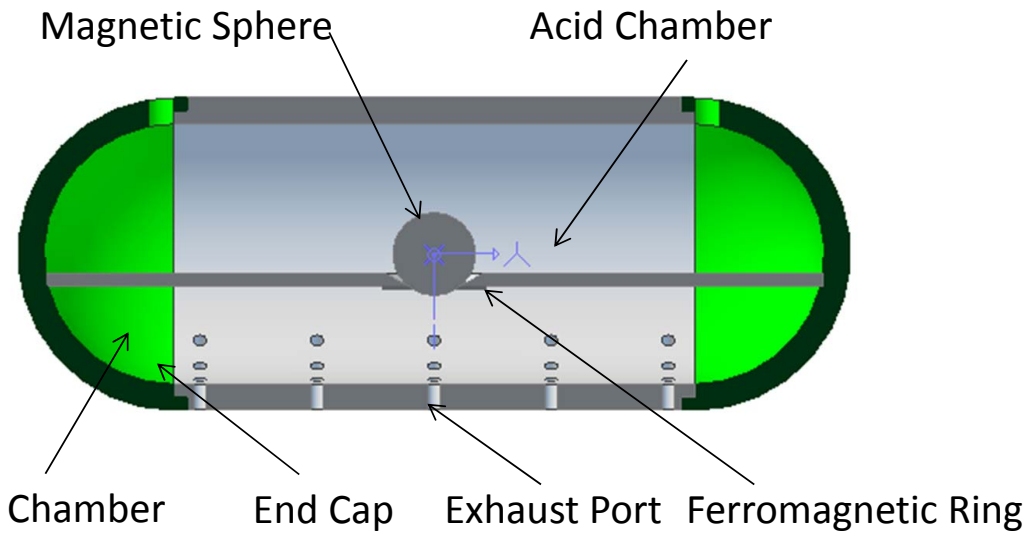

Figure 4.6: Sectional view of the internal wireless insufflation capsule body (12mm diameter by 32mm length), dividing wall (0.5mm thick), magnetic sphere (3.2mm diameter) and ferromagnetic ring (4.173 mm OD, 1.27mm ID, 0.1mm thick).

the magnetic sphere will align with the orientation of the external field.

Initial benchtop testing found that the magnetic ball valve could be actuated from a distance of approximately 6cm when using a 2" diameter by 2" thick, grade N52, axially magnetized, permanent magnet (K&J Magnetics, Inc. Model number DY0Y0-N52). Based on the dimensions of the capsule's chambers, the lower chamber is theoretically capable of holding 1.4g of Potassium Bicarbonate. Using the optimal volumetric water-to-reactant ratio of 0.5 identified in Section 3.2 this mass of potassium bicarbonate should be reacted with 0.90g of citric acid and 0.60mL of H_2O. Results presented in Section 3.2 indicate that said reactants should produce approximately 265mL of gas. Because the macroscopic density of powdered potassium bicarbonate proved to be less than the density associated with its characteristic crystal structure, in practice it was found that the initial version of the IRC was capable of

holding approximately 0.75g of potassium bicarbonate. Following initial qualitative assessments, it was discovered that damp, but unreacted, powder remained in the capsule's lower chamber long after output ceased to be generated. This may suggest that gas generation was hampered by inadequate mixing of citric acid solution and powdered potassium bicarbonate. In an effort to enhance mixing of the reactants, a second IRC prototype was developed.

Figure 4.7: First generation IRC prototype (12mm diameter by 32mm length), dividing wall (0.5mm thick), magnetic sphere (3.175mm diameter) and ferromagnetic ring (3.73mm OD, 1.27mm ID, 0.01mm thick).

4.3.2 Internal Reaction Capsule: Version Two

The design of the second IRC looked to promote more efficient mixing of the powdered base and acidic solution through the use of an additional ball valve. The prototype,

shown in Figure 4.8, incorporated a ball valve at each end of the capsule to allow citric acid solution to disperse through the powdered potassium bicarbonate more evenly.

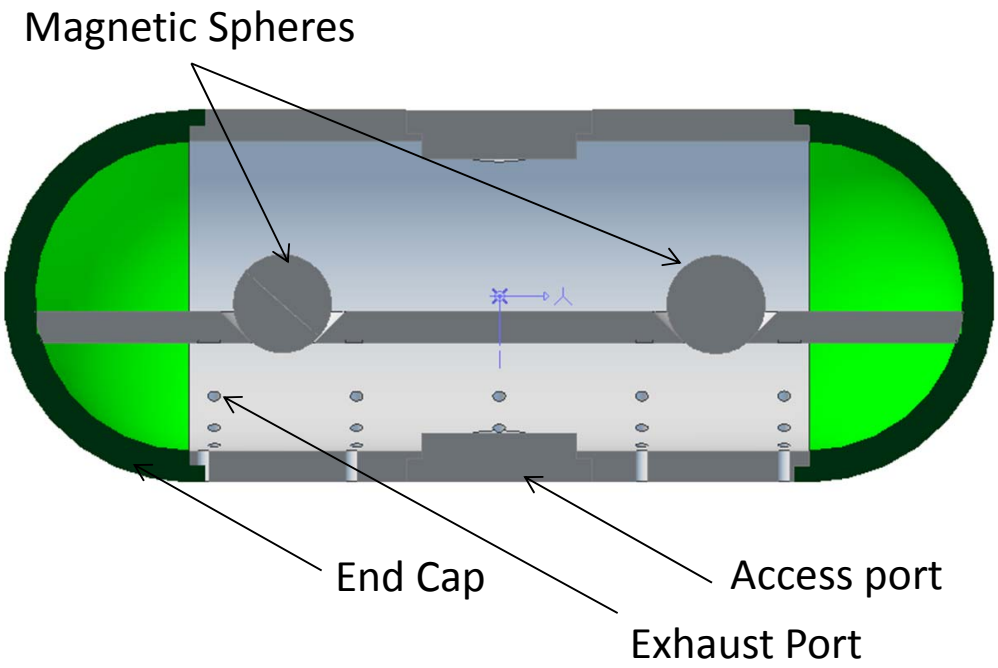

Figure 4.8: Sectional view of the second generation Internal Reaction Capsule body (12mm diameter by 32mm length), dividing wall, magnetic spheres and ferromagnetic rings.

With the relative dimensions of the capsule remaining unchanged, the capsule's base-carrying capacity remained the limiting factor on the output of the device. When the capsule is loaded with 0.75g of base, results presented in Section 3.2 indicate that the resulting output should be on the order of 140mL. Benchtop tests using the experimental setup outlined in Section 3.1 were conducted to determine if the capsule was capable of generating such an output. During these test, the capsule was activated in an initially dry environment. After a period of five minutes, a syringe was used to introduce 3mL of water. This was done to allow for the initial reaction of

the pill to be observed while also providing insight into the total output the capsule might yield in a wet environment. When the capsule was activated in dry conditions, the average output was 36mL ($\sim$ 31% efficiency).

During the benchtop trials it was observed that the initial pressure spike occurring at the start of the reaction often caused citric acid solution to be ejected from the capsule's upper chamber and, in some cases, powdered base was seen being ejected from the exhaust ports of the lower chamber. When the total mass of potassium bicarbonate in the lower chamber was reduced to 0.6 grams and 0.4grams the average output efficiency was found to increase to 44% and 55%, respectively. This trend seems to indicate that deceasing the relative volume of potassium bicarbonate in the lower chamber may mitigate the loses associated with high initial pressures in the capsule. In all cases, following the introduction of 3mL of water, the output produced after five minutes was found to meet or exceed expected values.

Results from the current trial seem to indicate that initial pressure can cause a loosely packed capsule to eject powdered base and/or citric acid solution. In the presence of standing water these expelled reactants will eventually react to produce the anticipated levels of gas. However, since much of the yield is still produced outside the capsule, it is likely this may still result in the formation of foam within the colon. In an effort to produce an IRC that contains the reaction within the interior of the capsule, a third and final version of the IRC was developed. The design and performance of said capsule is presented in the section that follows.

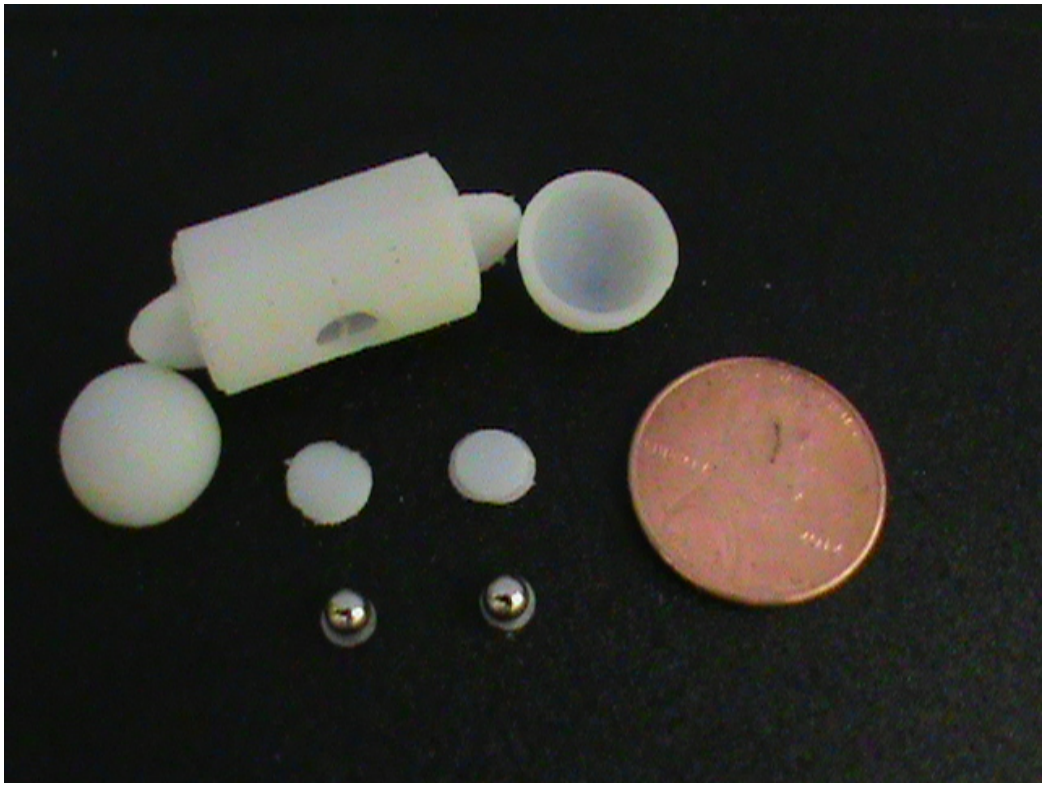

Figure 4.9: Various components of second generation internal reaction capsule including capsule body (12mm diameter by 32mm length), dividing wall (1mm thick), magnetic spheres (3.2mm diameter) and ferromagnetic rings (4.173 mm OD, 1.27mm ID, 0.1mm thick).

4.3.3 Internal Reaction Capsule: Version Three

The third generation of the IRC looks to mitigate the problems seen in previous version regarding initial pressures causing reactants to be ejected from the capsule. The current design attempts to accomplish said task by confining the magnetic spheres, which are used as ball valves, within separate chambers so as to allow them both to be reseated upon removal of the valve-actuating external field. A CAD rendering of the devise is shown in Figure 4.10. It is hypothesized that this action will allow flow within the capsule to be throttled in a manner that allows the initial pressure spike to be controlled. Additionally, where previous versions of the device had exhaust ports

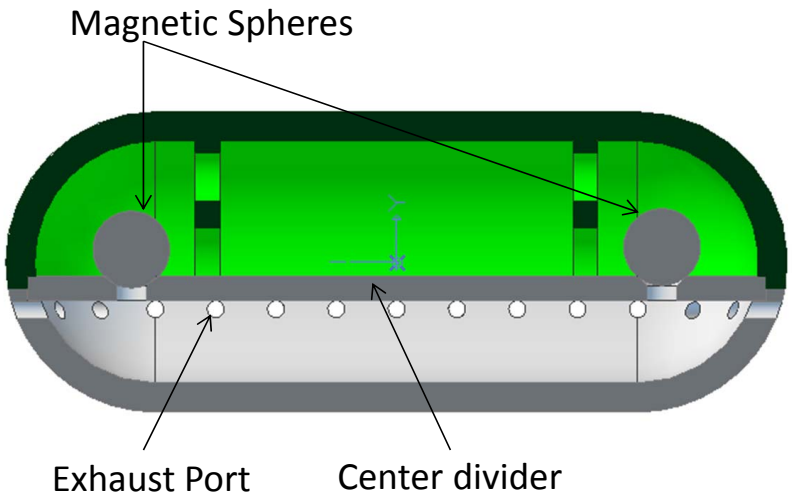

Figure 4.10: Sectional view of the third generation Internal Reaction Capsule body (12mm diameter by 32mm length), dividing wall (1mm thick), magnetic spheres (3.175mm diameter) and ferromagnetic rings, not shown (3.73mm OD, 1.27mm ID, 0.01mm thick).

in a radial pattern around the radius of the lower chamber of the capsule, the current design has exhaust ports located along the upper edge of the lower chamber. It is thought that this change in placement will help keep the powdered contents of the lower chamber within the capsule since avenues of escape are now located above said powdered contents rather than below.

The output produced by the current design was assessed using the benchtop setup described in Section 3.1. During these trials the capsule was loaded with 0.8 grams of potassium bicarbonate and 0.9mL of citric acid solution having a mass concentration of 1.5g/mL. In each trial, the capsule was activated in a dry 25mL flask and allowed to react for a period of five minutes. At that time, 3mL of room temperature H_2O were injected into the flask to mimic the moist environment of the colon. The output generated during the test was recorded at one minute intervals. As can be seen

Figure 4.11: Components (left) of third generation Internal Reaction Capsule body (12mm diameter by 32mm in length), dividing wall (1mm thick), magnetic spheres (3.175mm diameter) and ferromagnetic rings, not shown (3.73mm OD, 1.27mm ID, 0.01mm thick) and assembled device (right).

in Figure 4.12, output from the devices seems to reach a plateau at approximately 90mL as the five minute mark is approached. Following the introduction of H_2O in the reaction flask, the rate at which gas is produced is seen to initially increase and a new plateau is approached around the 150mL level. While total output produced by the third generation capsule is similar to that observed for the second generation capsule, the output generated prior to the introduction of the H_2O was found to be approximately twice the volume produced by the second generation design.

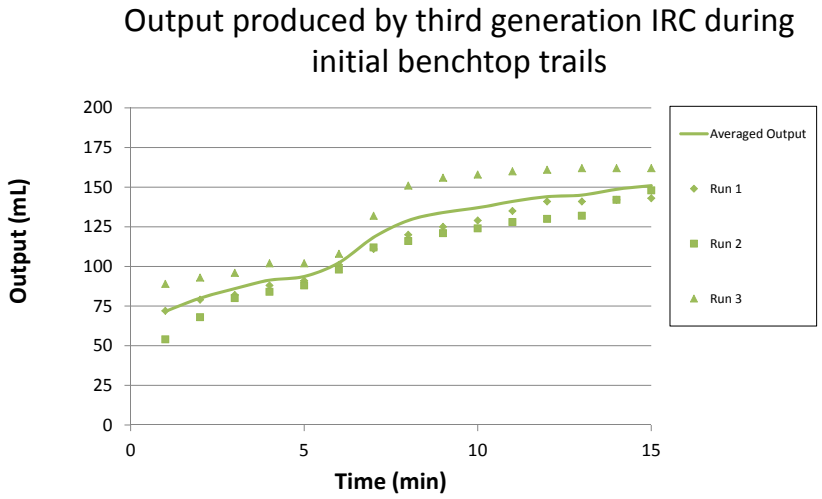

Figure 4.12: Transient output produced by third generation internal reaction capsule with average initial mass of potassium bicarbonate equal to 0.8 grams and an initial volume of 0.9mL of citric acid solution having a mass concentration of 1.5g/mL.

4.3.4 Internal Reaction Capsule: Ex-Vivo Trials

In order to assess feasibility of the IRC, two ex-vivo trials we undertaken. In both trials, the experimental setup shown in Figure 4.3, and described in Section 4.2.1, was used. In the first trial, a single capsule was placed approximately ten centimeters past the ring of markers furthest from the rectum. A robot arm was then used to position an external permanent magnet, in order to activate the capsule. The robotic arm was equipped with an ATI Mini 45 load cell to allow for force-control based manipulation of the magnet's location and orientation. In order to limit the displacement caused by the magnetic link between external permanent magnet and those used on-board the capsules, a thin piece of acrylic (approximately 3mm in thickness) was placed on top of the heated bath. During the trials, an endoscope (Karl Storz) was used to observe

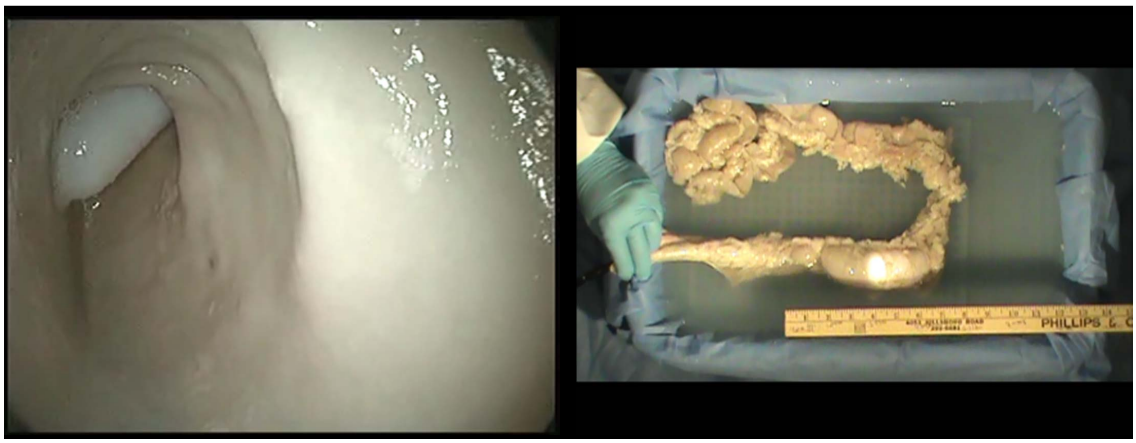

Figure 4.13: Endoscopic view (left) and external view (right) demonstrating the level of insufflation provided by a single third generation IRC approximately two minutes after activation.

the level of insufflation provided by the device and the amount of foam produced. The images presented in Figure 4.13 were taken approximately two minutes after the IRC was activated. As can be seen in the figure, the capsule was successful in locally inflating a section of colon measuring approximately 5.5 inches in length by one and a quarter inches in diameter. The figure also shows that foam generated by the capsule did not hamper the ability to view the colon lining in the area directly surrounding the capsule.

In the second trial, three capsules were placed approximately ten centimeters past the ring of markers furthest from the rectum. Once again, a robotic arm equipped with a axially-magnetized cylindrical end-effector was used to activate the capsules by simply passing over the length of the colon while remaining roughly four inches above the water level of the heated bath. Figure 4.14 shows an image taken with the endoscope (left) and an exterior view of the colon (right) that were taken approxi-

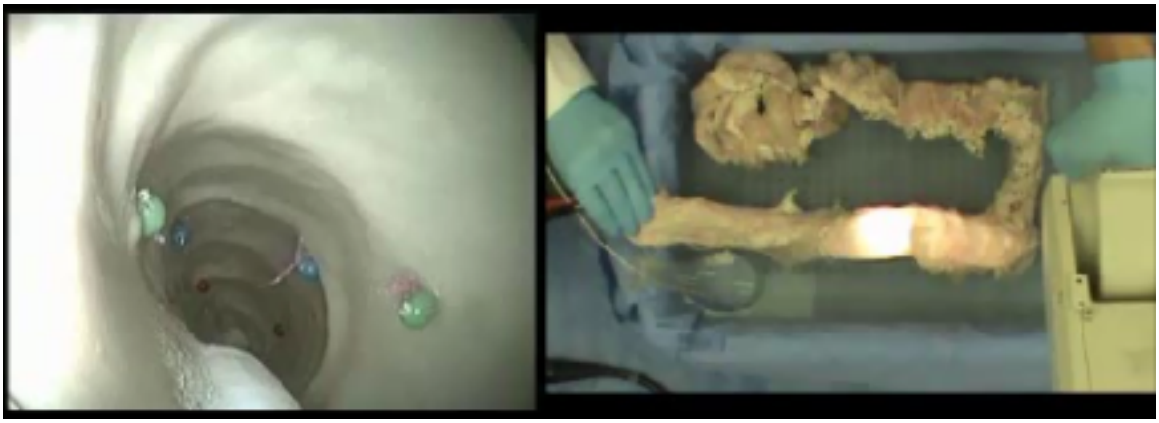

Figure 4.14: Endoscopic view (left) and external view (right) demonstrating the level of insufflation provided by three third generation IRC's approximately one minute after activation.

mately one minute after the initial activation. As can be seen in the figure, one of the capsules has been pulled away from the other two by the magnetic force developed during the initial activation. While a small amount of foam can be seen exiting the capsule, the image demonstrates that after as little as one minute the capsules were able to provide enough insufflation to allow for visualization of six markers, and two capsules, disbursed over a section of colon measuring approximately five inches in length.

Approximately three minutes after the initial activation, the external permanent magnet was used to activate the capsules once again. During this event, the magnetic attraction developed between various components in the system caused the three capsules to come together between the second and third rings of markers. Figure 4.15 shows the capsules being held against the upper side of the colon wall and the foam produced by the reaction during this dynamic event. Figure 4.16 provides interior and exterior images of the colon taken approximately two minutes after the

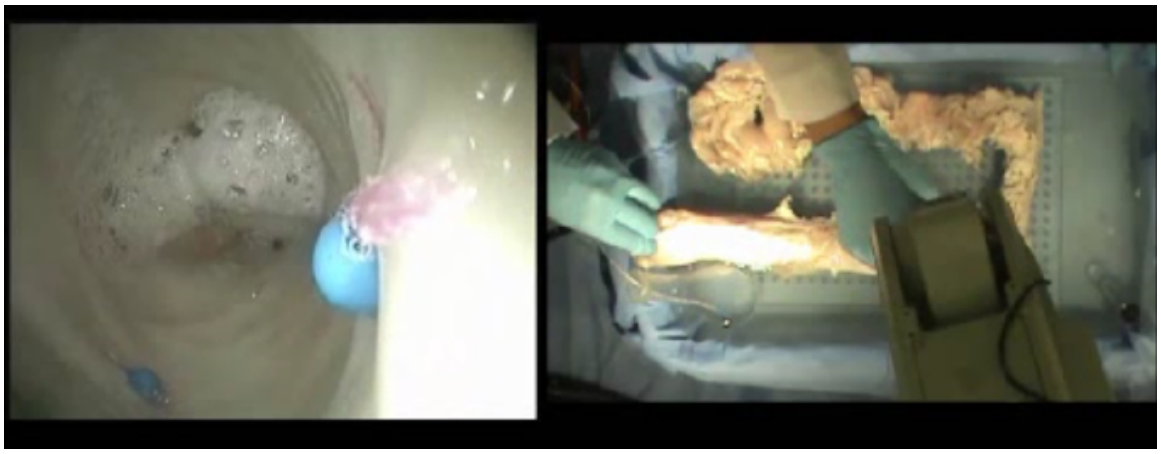

Figure 4.15: Endoscopic view (left) and external view (right) during a secondary activation of three IRCs approximately two minutes after an initial activation during the same ex vivo trial

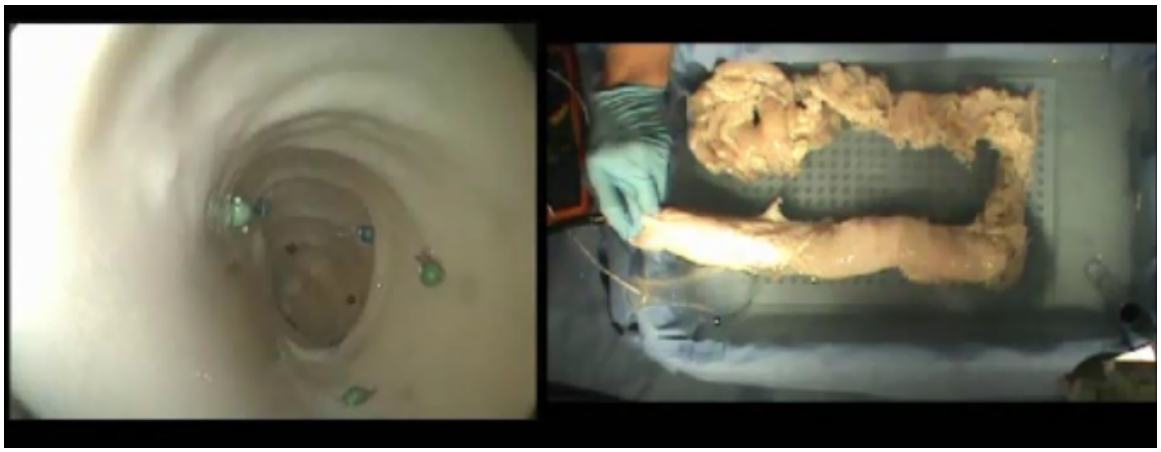

Figure 4.16: Endoscopic view (left) and external view (right) demonstrating the level of visualization provided by three third generation IRCs approximately one minute after a secondary activation.

second activation of the capsules. As can be seen in the figure, approximately five minutes after the initial activation, and two minutes after a subsequent activation, visualization within the colon has been greatly enhanced. This demonstrates that even after a dynamic triggering of the capsules, potassium bicarbonate and citric acid can be used to provide foam-free enhancement of both visualization and locomotion within the colon.

Chapter 5

Discussion

Insufflation has a two-fold clinical value in capsule endoscopy. First, it has the potential to enhance visualization, especially in larger lumens such as the colon. Second, it can ease the passage of active locomotion capsules, whether they be actuated by externally applied magnetic fields or other methods, such as legs, when they might otherwise be impeded by deflated intestinal folds. As shown in this study, even a small amount of insufflation substantially increases the surface area of the intestine that is visible to the capsule since gases tend to form a local bubble of inflated intestine close to the source of insufflation. This enhanced visualization could improve a capsule endoscope's sensitivity for detecting colonic polyps, advanced adenomas, and colorectal cancer, which is currently relatively low compared to traditional colonoscopy. While results show it is possible to carry a sufficient volume of reactants onboard a single capsule to locally enhance visualization and locomotion, one can easily envision how such a capsule could be used as part of a multiple capsule solution similar to the three inflation capsules plus camera experiment in Chapter 4. In such a system, one or more capsules could provide insufflation while other capsules are used to acquire images, provide diagnostic functions, or deploy therapeutic intervention.

5.1 Choice Of Working Reaction

The present work has presented a wireless system to inflate the colon through the use of a biocompatible chemical reaction. The proposed solution entails the use potassium bicarbonate and citric acid. The achieved volume of gas has been found sufficient to

distend the colon lumen. This inflation produces a tangible enhancement of colon lining visualization. While not presented in this work, not yet published preliminary experiments indicate that, environmental conditions have marked effect on the yield of gas. Temperature is particularly important, since it enhances chemical solubility and reaction kinetics. In fact, an incremental yield of 26.6% and 33.96% has been found for the reactions with potassium bicarbonate and sodium bicarbonate, respectively, when comparing room temperature gas generation with the yield obtained at 37^{o}C.

In the present work, carbon dioxide is the product responsible for inflation. This gas is easily absorbed through the internal mucosa into the blood, and its use avoids overdistention and post-procedure abdominal discomfort [45]. The reaction between potassium bicarbonate and citric acid has been found to generate the largest output. However, this reaction produces potassium citrate and should therefore not be used in cases of patients presenting with kidney failure or urinary infection. In such cases, the reaction with sodium bicarbonate should be used since potassium citrate or potassium bicarbonate absorbed by the colon [46] could aggravate these conditions.

While the results presented in this work indicate that the reactions used have the potential to obscure a capsule endoscope's view of the colon due to the production of foam, one can envision a scenario where said foam is used to disperse dyes in a manner akin to chromoendoscopy [47]. Chromoendoscopy is the practice of using adsorptive, contrast or reactive chemical agents to provide greater contrast between healthy tissue and abnormalities. In the case of capsule based endoscopy, the reactants could be premixed with indigo carmine to allow an IRC to release dye-infused foam throughout the colon prior to inspection with a WCE. Studies concerning the clinical relevance

of chromoendoscopy have reported site-dependent results, indicating that the technique may depend considerably on the operator [47]. It therefore stands to reason that incorporating chromoendoscopy in a robotic-based WCE platform could remove operator dependencies and provide the advantage associated with chromoendoscopy to a larger number of patients.

5.2 Capsule Design

While the present work has presented four capsule designs, these prototypes represent a body of knowledge that was gained during the design and fabrication of more than fifty unique designs. Many of the preliminary capsules, which have not been included in this work for brevity, incorporated the use of custom microcontrollers, commercially available valves and reed switches, precision machined components, and state-of-the-art power supplies. While the design and fabrication of said capsules provided ample opportunity to demonstrate technical prowess, benchtop testing proved time and again that simpler systems outperformed their more complex counterparts. A likely reason for these findings can be found in the inherent limitations imposed by current 3D printing technology. While the systems used during this work are capable of printing features less than half a millimeter in principal dimension, features on this scale are often hard to post process after they are printed and their limited surface area makes adhesion challenging even when working with epoxies specifically formulated for use with the types of polymers that are used by 3D printers.

One example of an early prototype which incorporates electromechanical activation and precision fabrication is presented in Figure 5.1. In theory, this hydrogen

peroxide based insufflation capsule could be activated by a physician by simply using a magnet to close a magnetic reed switch. When the reed switch is closed, current from the battery flows through a high resistance wire. The heat generated by the resistive load serves to melt a paraffin wax plug. Prior to heating, this plug is used to restrain the forward motion of the system's catalyst containment sled as it is being acted on by the force of a compressed spring. When the wax is heated to a point where it's shear strength can no longer support the load provided by the spring, the catalyst containment sled translates forward. While the catalyst containment sled cover prevents hydrogen peroxide from entering the catalyst containment sled prior to activation, following the translation, flow in and out of the containment sled is unimpeded and the reaction commences. While hydrostatic tension prevents hydrogen peroxide from escaping the pill, once the hydrogen peroxide is converted to oxygen, it is free to pass through said holes so it may inflate the colon.

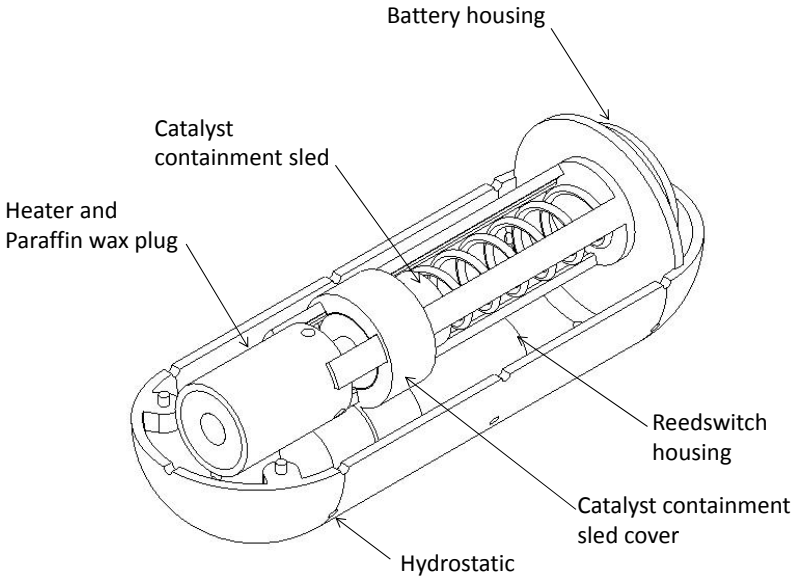

Figure 5.1: Early electromechanical H_2O_2 capsule prototype.

Realization of the design shown in Figure 5.1 requires a number of engineering skill sets. Sizing of the paraffin wax support requires a working knowledge of mechanics of materials. Ensuring that the resistive heater can melt the paraffin wax requires insight into passive electronics and heat transfer. Maximizing the design's fluid carrying capacity can be achieved by minimizing the volume required of internal structures with the aid of finite element analysis. All of these skills were utilized in the development of the capsule. Despite the number of technical hurdles that were overcome to realize said design the challenges presented by reliably sealing the chambers containing electrical components, and the two halves of the capsule, proved to be nontrivial, to say the least. In an effort to overcome these challenges, subsequent variations of this concept employed magnetic components in lieu of electromechanical components since the former can be exposed to hydrogen peroxide without fear of

failure. An example of a magnetic-based insufflation capsule which arose from the lessons learned during early electromechanical designs is presented in Figure 5.2.

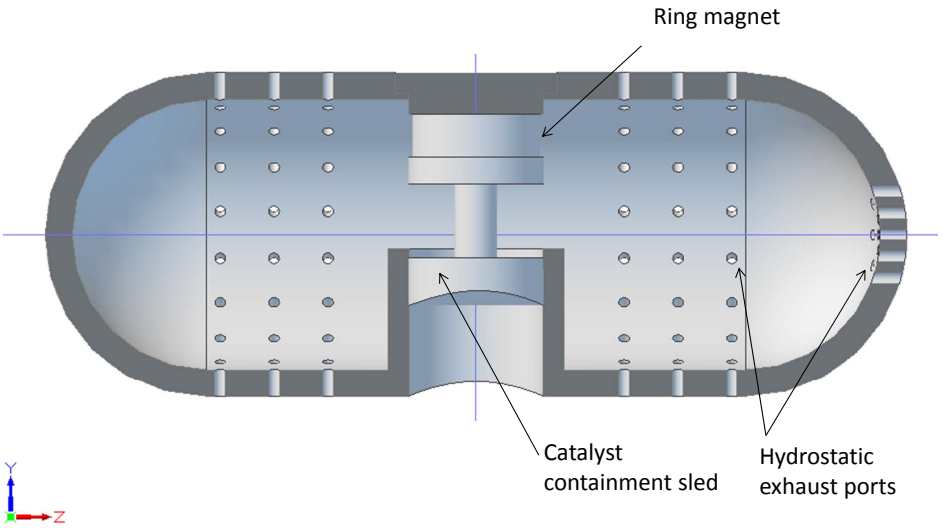

Figure 5.2: Early magnetic H_2O_2 capsule prototype.

Figure 5.2 shows a magnetic-based insufflation capsule. In said concept, hydrogen peroxide is stored in the body of the capsule while a small chamber within the capsule is used to house the catalyst. The capsule is triggered by using an external magnet to induce a force on an internal magnet which is attached to the catalyst chamber. This force causes the catalyst chamber to be translated into the center of the capsule where the catalyst is exposed to the hydrogen peroxide within the body of the capsule. This concept eliminates the need for electronic components and thereby mitigates issues associated with insulating said components from fluids within the capsule. That said, the geometry associated with the catalyst containment sled and the tolerances associated with the rapid prototyping system made it difficult to achieve effective

sealing between the catalyst containment chamber and the interior of the capsule when attempting to execute this concept. Subsequent concepts overcame this sealing challenge by employing flat-on-flat interfaces for sealing surfaces. An example of such a design is given by Figure 5.3.

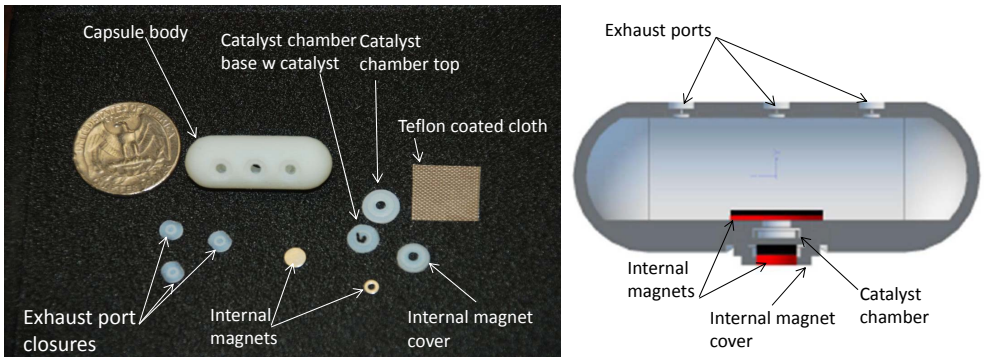

Figure 5.3: Picture (left) and cad rendering (right) of a revised magnetic H_2O_2 capsule concept demonstrating flat-on-flat valve sealing.

The capsule shown in Figure 5.3 uses a small catalyst containment chamber, two internal magnets and simple interface geometry to ensure reliable valve seating capable of withstanding the aggressive nature of high concentration hydrogen peroxide. While the final design of the IRC used a single spherical magnet paired with a ferromagnetic ring to provide the necessary sealing force, the original IRC concept utilized the style of valve shown in Figure 5.3. While the flat-on-flat valve design allows for reliable and robust valve seating due to the high tolerances that can be achieved when manufacturing such simple geometry, the valve design utilized in versions of the IRC presented in Chapter 4 looked to maximize the volume available of reactants by minimizing the volume required for internal structures. Hydrogen peroxide based in-

sufflation capsule designs were not presented in Chapter 4, nor were ex-vivo trials ever undertaken, due to the health risk associated with such a reactive solution, however, it is worth noting that many of the design features ultimately incorporated in the acid/base prototypes were derived from lessons learned while exploring the feasibility of H_2O_2 based WCI.

The extensive number of design iterations undertaken during this work served to highlight a number of design principles which proved particularly advantageous when developing capsule based devices. Paramount amongst said principles is the need to keep designs as simple as possible. While it may be natural for an engineer to want to display as many of their technical competencies as possible in a given design, the volume restrictions placed on capsule endoscopy leaves little room for showing off. A number of very impressive capsules have been developed through the use of advanced design and machining however, the complexity associated with such capsules severely limits the likelihood of reaching mass markets. Furthermore, reducing the complexity of a capsule often allows for enhanced functionality. In the case of WCI this lesson is exemplified by the increases in reactant volume which can be obtained by eliminating the need for electronics, power supplies, and the housing structures that would otherwise be necessitated by said components.

The other design principles elucidated during the extensive number of design iterations undertaken during this work build on the concept of simplicity. While post processing and assembly may require a design to broken down into a number of different pieces, whenever possible, the total number of pieces utilized in a given assembly should be kept to a minimum. Inevitably, each piece in an assembly will need to

be contained within the assembly. While this may be accomplished with the use of adhesives or kinematically inspired design features, incorporation of either will undoubtedly require greater volume than might otherwise be used if the component were integrated into a larger structure. As previously stated, post processing, and in some cases assembly, will place limitations on the number of features that can be consolidated into a given structure, so one should try to remain mindful of the cost and benefits associated with breaking a larger structure down into smaller constitutive components.

Finally, while the capabilities of modern 3D printers allow for the fabrication of astonishingly small components, the effort required for the post processing and assembly of such components is often inversely related to their scale. This provides yet another reason to consolidate smaller components into larger sub-assemblies whenever possible.

5.3 Future Work

During the present work it was observed that the macroscopic density of the powdered reactants was about half of the manufacturer's stated density. While efforts were made to compact powdered reactants as they were being loaded into the capsules, future work will investigate the use of hydraulic compaction to obtain densely packed reactants in a form factor matching that of the capsule's inner chambers. It is thought that such a technique will allow for greater yields by increasing the mass of reactants that can be loaded into a given volume and by reducing the likelihood of reactants being ejected from the capsule during periods of high internal pressure.

Magnetic valve design presents another area for future research. In the present work, the IRC employed the use of magnetic spheres and ferromagnetic rings to produce a ball valve capable of being actuated by an external magnetic field source. While the valves were found to operate sufficiently to provide for a proof of concept, several aspects of the valve could be optimized for the benefit of future designs. During testing, it was noted, the citric acid solution used by the IRC produced a sticky film that caused the valves to become stuck in the open position after repeated use. Future designs will investigate the use of anti-stick coating to prevent this action.

In the case of pairing WCI with magnetic-based active locomotion, the magnetic ball valve within the insufflation capsule should be designed such that an active capsule can be maneuvered past an insufflation capsule without resulting in a magnetic couple that is strong enough to cause the two to become linked. This could be accomplished by sizing the moving magnet within the insufflation capsule such that the force generated between it and other magnetic field sources within the system is less than the weight of the insufflation capsule. In such a case, an active capsule could be moved along the upper side of the colon wall while insufflation capsules lay on the lower surface.

The exhaust ports utilized in the IRC also represent a design feature which could be optimized in future iterations. In the final IRC design the exhaust ports were moved to the upper edge of the powdered reactant chamber in an effort to prevent said reactant from being expelled from the chamber by high initial pressures. Another method that could enhance flow through the capsule while retaining reactants within may be realized through the uses of a hydrophobic coating around the exhaust ports in

the upper chamber of the capsule. While the polypropylene-like material the current prototypes were constructed of renders the capsules hydrophilic, the upper chamber of the capsules could be treated with a hydrophobic coating, like paraffin wax, such that small openings in the capsule's shell would allow gases to exit the capsule while providing resistance to passing liquids.

Future work will also look to assess the system's performance in an animal-based in vivo model. While the use of a porcine model for said purposes will not take into account the challenges that may be presented by haustral folds, it will certainly provide a preliminary proof-of-concept in an in vivo setting. Subsequent animal and human trials will require comparison with standard colonoscopy, to quantitatively assess the effectiveness of WCI when acting as part of modular capsule endoscopy platform.

Appendix A

H_2O_2 Decomposition

The decomposition of H_2O_2 to produce dioxygen and water is given by

$$2H_2O_2 \rightarrow 2H_2O + O_2 \tag{A.1}$$

showing that each mole of H_2O_2 decomposes to produce two moles of water and half a mole of dioxygen. Given a desired initial volume of H_2O_2, the mass of H_2O_2 solution needed, for a given concentration, is given by

$$V_{tot} = X * (w_{H_2O_2} * \frac{1}{\rho_{H_2O_2}} + (1 - w_{H_2O_2}) * \frac{1}{\rho_{H_2O}}) \tag{A.2}$$

Where $w_{H_2O_2}$ is the mass fraction of hydrogen peroxide in the solution, i.e. the mass of hydrogen peroxide divided by the total mass of the solution. The total mass of the solution is denoted by X and the mass of H_2O_2 found in the solution is given by

$$m_{H_2O_2} = X * w_{H_2O_2} \tag{A.3}$$

and the total number of H_2O_2 moles is given by

$$Mol_{H_2O_2} = \frac{m_{H_2O_2}}{MM_{H_2O_2}} \tag{A.4}$$

As previously stated, one mole of H_2O_2 decomposes to form two moles of H_2O and half a mole of O_2. Therefore, if we estimate the volume of gas produced by setting it equal to the volume occupied by a given number of O_2 moles, the volume of gas generated is given by

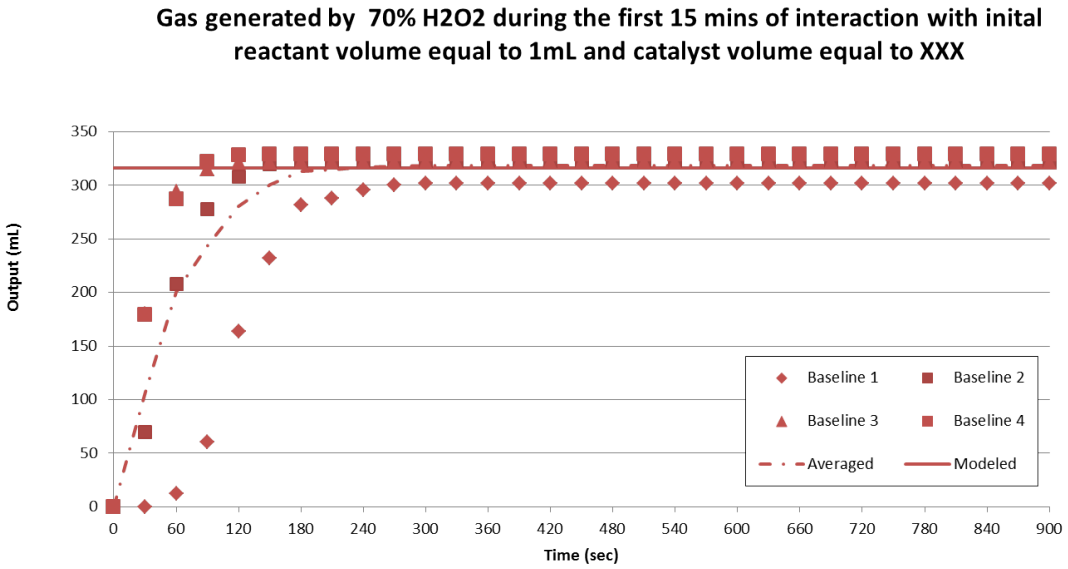

Figure A.1: Output generated as a function of time when decomposing 1mL of 70% H_2O_2 using approximately 0.5 mL of iridium .

$$V_{generated} = \frac{1}{2} Mol_{H_2O_2} * \frac{MM_{O_2}}{\rho_{O_2}} \tag{A.5}$$

For the case of 1mL of 70% H_2O_2, this model predicts an output of approximately 316.042mL when using the molar mass and density of dioxygen as given in Table B.1. As can be seen from the results presented in Figure A.1 when 1mL of 70% H_2O_2 is decomposed using a small volume of iridium pellets the modeled and experimental results find good agreement.

Appendix B

Acid-Base Reactions

Acids and bases are commonly defined by the cation and anion they produce in the presence of water. When acids are added to water they produce hydrogen ions, H^+, while bases produce hydroxide ions, OH^-, in the presence of water. While acids react with some metals to produce hydrogen, H_2 , they also react with compounds containing CO_3^{2-} to form water and carbon dioxide. Given the biocompatibility of this latter group of products, their use will be investigated in the present work.

In order to estimate the amount of gas a given acid/base reaction may generate we can start by determining the number of moles of each that could be delivered in a capsule of known volume.

$$V_{tot} = X_{molesacid} * \frac{MM_a}{\rho_a} + Y_{molesbase} * \frac{MM_b}{\rho_b} \tag{B.1}$$

Where V_{tot} is the total volume available for reactants. The molecular mass of the acid and base are given by MM_a and MM_b, respectively. The density of the acid and base are given by ρ_a and ρ_b, respectively.When the ratio of acid moles to base moles is known, equation B.1 can be rewritten as

$$V_{tot} = X_{molesacid}(\frac{MM_a}{\rho_a} + R * \frac{MM_b}{\rho_b}) \tag{B.2}$$

where $R = Y_{molesbase}/X_{moleacid}$. The value of R can be determined by balancing the number of hydrogen ions, H^+, and hydroxide ions, OH^-, present in the initial reactants and the mass of the initial reactants can then be determined by

$$mass_a = MM_a \frac{V_{tot}\rho_a\rho_b}{MM_a\rho_b + MM_bR\rho_a} \tag{B.3}$$

and

$$mass_b = MM_bR \frac{V_{tot}\rho_a\rho_b}{MM_a\rho_b + MM_bR\rho_a} \tag{B.4}$$

If we specify a generic acid structure as HA, where A^- is an anion, and a generic base structure as BOH, where B^+ is an appropriate cation, then, in generic terms, an acid/base reaction can be give as

$$H^+ + A + B + OH^- \rightarrow A + B + H_2O \tag{B.5}$$

where H_2O often results due to the highly favorable bonding configuration offered by $H^+ + OH^-$. This pair occurs stoichiometricly when the number of H^+ cation produced by the dissociation of HA compounds matches the number of OH^- anions result from the dissociation of BOH compounds. The nature of the initial HA and BOH structures will therefore have an effect on the ratio needed for stoichiometric production of H_2O, and hence CO_2. As an example, consider the familiar vinegar and baking soda volcano. Otherwise known as an acetic acid and sodium bicarbonate volcano.

When acetic acid, CH_3CO_2H, and sodium bicarbonate, $NaHCO_3$, are dissolved in water, they disassociate to form an acetate ion and a hydrogen ion ($C_2H_3O_2^- + H^+$) and a sodium ion, carbon dioxide and a hydroxide ion ($Na^+ + CO_2 + OH^-$), respectively. These reactants result in the production of sodium acetate, water and

carbon dioxide. With a mole-to-mole ratio of unity, this reaction is given by

$$CH_3COOH + NaHCO_3 \rightarrow CH_3COO^- + H^+ + Na^+ + CO_2 + OH^- \tag{B.6}$$

$$\rightarrow CH_3COONa + CO_2 + H_2O \tag{B.7}$$

and equation B.2 becomes

$$X_{molesacid} = \frac{V_{tot}}{(\frac{MM_a}{\rho_a} + \frac{MM_b}{\rho_b})} \tag{B.8}$$

Since the number of moles of CO_2 produced by this reaction is equal to the number of moles of base initially provided, the volume of the volume of CO_2 produced is given by

$$V_{CO_2} = \frac{V_{tot}}{(\frac{MM_a}{\rho_a} + \frac{MM_b}{\rho_b})} \frac{MM_{CO_2}}{\rho_{CO_2}} \tag{B.9}$$

If we turn our attention to the less ubiquitous citric acid and sodium bicarbonate reaction, we see that citric acid disassociates into a citric acid ion ($C_6H_5O_7^{-3}$) and three hydrogen ions ($3H^+$). When this solution is reacted with sodium bicarbonate they must be mixed in a 3-to-1 molar ratio since each sodium bicarbonate molecule will disassociate to from only one hydroxide ion. This process, which results in the production of sodium citrate ($C_6H_5Na_3O_7$), carbon dioxide (CO_2) and water (H_2O), is given by

$$C_6H_8O_7 + 3NaHCO_3 \rightarrow C_6H_5O_7^{-3} + 3H^+ + 3Na^+ + 3CO_2 + 3OH^- \quad \text{(B.10)}$$

$$\rightarrow C_6H_5Na_3O_7 + 3CO_2 + 3H_2O \quad \text{(B.11)}$$

While the preceding examples illustrate how the structure of the acid molecule will have a direct effect on the number of CO_2 moles produced, this model does not account for the effect that properties such as density, solubility and heat of formation have on the total volume of the products. Given these unaccounted variables, experimental results are used to validate the response of the model for all possible acid/base combinations arising from the use of acetic and citric acid and sodium bicarbonate and potassium bicarbonate. Having determined the proper molar ratio for reacting acetic acid with sodium bicarbonate, and citric acid with sodium bicarbonate, we now look to determine the proper ratio for stoichiometrically reacting acetic acid with potassium bicarbonate and citric acid with potassium bicarbonate.

When potassium bicarbonate is dissolved in water it disassociates to form a potassium ion (K^+), carbon dioxide (CO_2) and a hydroxide ion (OH^-). Due to the production of a single hydroxide ion per molecule of potassium bicarbonate, this base can be reacted in a one-to-one molar ratio with acetic acid, to give

$$CH_3COOH + KHCO_3 \rightarrow CH_3COO^- + H^+ + K^+ + CO_2 + OH^- \quad \text{(B.12)}$$

$$\rightarrow CH_3COOK + CO_2 + H_2O \quad \text{(B.13)}$$

or, it can be reacted in a three-to-one molar ratio with citric acid to give

$$C_6H_8O_7 + 3KHCO_3 \rightarrow C_6H_5O_7^{-3} + 3H^+ + 3K^+ + 3CO_2 + 3OH^- \quad \text{(B.14)}$$

$$\rightarrow C_6H_5K_3O_7 + 3CO_2 + 3H_2O \quad \text{(B.15)}$$

As can be seen from inspection of equations B.6-B.7 and B.10-B.15 in the case of acetic acid being reacted with the given bases, one mole of acid results in one mole of CO_2, while in cases when citric acid is used, one mole of acid results in three moles of CO_2. Given the molecular masses and densities listed in Table B.1, the expected volumes produced from given initial reactant volumes can be calculated using equation A.9 along with the proper molar ratio, R. Results produced by the model are shown in Figure B.1.

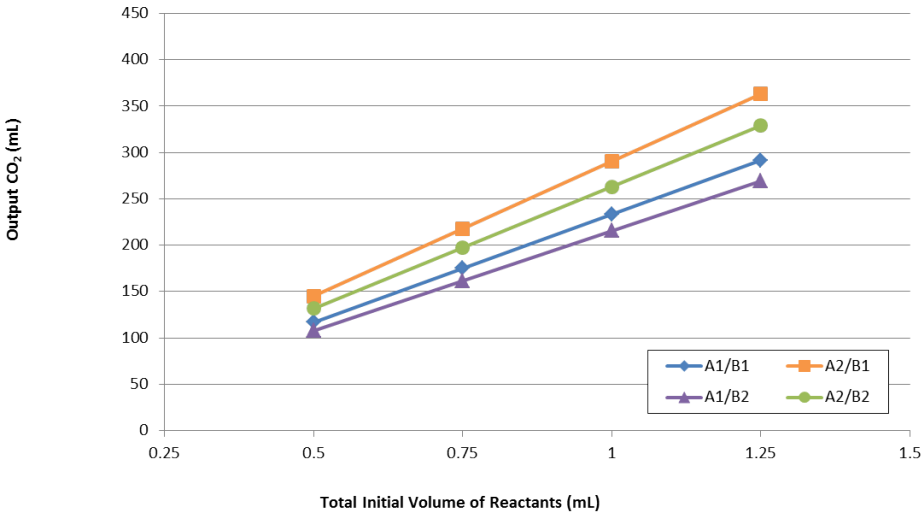

Figure B.1: Theoretical output from selected acid/base combinations

B.1 Reactant And Product Properties

Table B.1: Physical properties of various reactants and products at NTP

Chemical	Molecular Mass (g/mol)	Density (g/mL)
Acetic Acid	60.05	1.049
Citric Acid	192.12	1.665
Sodium Bicarbonate	84.01	2.2
Potassium Bicarbonate	100.115	2.17
Carbon Dioxide	44.01	$1.842 * 10^{-3}$
dioxygen	32	$1.331 * 10^{-3}$

Bibliography

[1] M. Classen, *Gastroenterological Endoscopy*. Thieme Medical Publishers, 2010.

[2] D. O. Faigel, *Endoscopic Oncology: Gastrointestinal Endoscopy And Cancer Management*. Humana Press, 2006.

[3] J. D. Conway, D. G. Adler, D. L. Diehl, F. A. Farraye, S. V. Kantsevoy, V. Kaul, S. R. Kethu, R. S. Kwon, and P. Mamula, "Endoscopic hemostatic devices," *Gastrointestinal Endoscopy*, vol. 69, no. 6, pp. 987–96, 2009.

[4] D. S. Ferreira, P. G. Coutinho, E. S. Castanheira, J. H. Correia, and G. Minas, "Fluorescence and diffuse reflectance spectroscopy for early cancer detection using a new strategy towards the development of a miniaturized system.," in *Annual International Conference of the IEEE Engineering in Medicine and Biology Society*, 2010.

[5] P. Valdastri, C. Quaglia, E. Susilo, A. Menciassi, P. Dario, C. N. Ho, G. Anhoeck, and M. O. Schurr, "Wireless therapeutic endoscopic capsule: in vivo experiment," *Endoscopy*, vol. 40, pp. 979–82, 2008.

[6] K. Kong, J. Cha, and D. Jeon, "A rotational micro biopsy device for the capsule endoscope," in *IEEE International Conference on Intelligent Robots and Systems*, 2005.

[7] P. Valdastri, M. Simi, and R. J. W. III, "Advanced technologies for gastrointestinal endoscopy," *Annual Review of Biomedical Engineering*, 2012.

[8] American Cancer Society, "What are the key statistics about colorectal cancer?,"

vol. http://www.cancer.org/Cancer/ColonandRectumCancer/DetailedGuide/colorectal-cancer-key-statistics, Last accessed June 2012.

[9] B. K. Edwards, E. Ward, B. A. Kohler, C. Eheman, A. G. Zauber, R. N. Anderson, A. Jemal, M. J. Schymura, I. Lansdorp-Vogelaar, L. C. Seeff, M. V. Ballegooijen, S. L. Goede, and L. A. G. Ries, "Annual report to the nation on the status of cancer, 1975-2006, featuring colorectal cancer trends and impact of interventions (risk factors, screening, and treatment) to reduce future rates," *Jounral of the National Cancer Institue*, vol. 103, pp. 1–23, 2011.

[10] W. AH, A. Paganini-Hill, R. K. Ross, and B. E. Henderson, "Alcohol, physical activity and other risk factors for colorectal cancer: A prospective study," *Journal of Cancer*, vol. 55, no. 6, pp. 687–94, 1987.

[11] D. W. West, M. L. Slattery, L. M. Robison, K. L. Schuman, M. H. Ford, A. W. Mahoney, J. L. Lyon, and A. W. Sorensen, "Dietary intake and colon cancer: Sex and anatomic site-specific associations," *American Journal of Epidemiology*, vol. 130, no. 5, pp. 883–94, 1989.

[12] W. C. Willett, M. J. Stampfer, G. A. Colditz, B. A. Rosner, and F. E. Speizer, "Relation of meat, fat, and fiber intake to the risk of colon cancer in a prospective study among women," *New England Journal of Medicine*, vol. 323, no. 24, pp. 1664–72, 1990.

[13] G. A. Kune, S. Kune, and L. F. Watson, "Colorectal cancer risk, chronic illnesses,

operations, and medications: Case control results from the melbourne colorectal cancer study," *Cancer Research*, vol. 48, no. 15, pp. 4399–404, 1988.

[14] C. Garland, R. Shekelle, E. Barrett-Connor, M. Criqui, A. Rossof, and O. Paul, "Dietary vitamin d and calcium and risk of colorectal cancer: a 19-year prospective study in men," *Lancet*, vol. 1, pp. 307–9, Feb. 1985.

[15] The American Cancer Society June 2012.

[16] N. Segnan, C. Senore, B. Andreoni, A. Azzoni, L. Bisanti, A. Cardelli, G. Castiglione, C. Crosta, A. Ederle, A. Fantin, A. Ferrari, M. Fracchia, F. Ferrero, S. Gasperoni, S. Recchia, M. Risio, T. Rubeca, G. Saracco, and M. Zappa, "Comparing attendance and detection rate of colonoscopy with sigmoidoscopy and fit for colorectal cancer screening," *Gastroenterology*, vol. 132, pp. 2304–12, JUN 2007.

[17] J. M. Inadomi, S. Vijan, and N. K. Janz, "Adherence to colorectal cancer screening: A randomized clinical trial of competing strategies," *Archives of Internal Medicine*, vol. 172, no. 7, pp. 575–582, 2012.

[18] A. V. Gossum, M. M. Navas, I. Fernandez-Urien, C. Carretero, G. Gay, M. Delvaux, M. G. Lapalus, T. Ponchon, H. Neuhaus, M. Philipper, G. Costamagna, M. E. Riccioni, C. Spada, L. Petruzziello, C. Fraser, A. Postgate, A. Fitzpatrick, F. Hagenmuller, M. Keuchel, N. Schoofs, and J. Deviere, "Capsule endoscopy versus colonoscopy for the detection of polyps and cancer," *New England Journal of Medican*, vol. 361, pp. 264–270, Jul 2009.

[19] The Center for Disease Control and Prevention, "Colorectal cancer screening basic fact sheet," vol. http://www.cdc.gov/cancer/colorectal/pdf/Basic_FS_Eng_Color.pdf, Last accessed June 2012.

[20] R. E. Davila, E. Rajan, T. H. Baron, D. G. Adler, J. V. Egan, D. O. Faigel, S. I. Gan, W. K. Hirota, J. A. Leighton, D. Lichtenstein, W. A. Qureshi, B. Shen, M. J. Zuckerman, T. VanGuilder, and R. D. Fanelli, "ASGE guideline: Colorectal cancer screening and surveillance," *Gastrointestinal Endoscopy*, vol. 63, no. 6, pp. 546–92, 2006.

[21] R. Li, J. Liu, H. Xue, and G. Huang, "Diagnostic value of fecal tumor m2-pyruvate kinase for crc screening: a systematic review and meta-analysis," *International Jounral of Cancer*, vol. 131, no. 8, pp. 1837–45, 2012.

[22] T. Wilkins, R. Gillies, D. M. Jester, and J. Kenrick, "The current state of flexible sigmoidoscopy training in family medicine residency programs," *Family Medicine*, vol. 37, pp. 706–11, 2005.

[23] T. Wilins and P. L. Reynolds, "Colorectal cancer: A summary of the evidence for screening and prevention," *American Family Physician*, vol. 78, no. 12, pp. 1385–92, 2008.

[24] P. J. Pickardt, "Incidence of colonic perforation at ct colonography: Review of existing data and implication for screening of asymptomatic adults," *Radiology*, vol. 239, pp. 313–39, 2006.

[25] A. Sonnenberg, F. Delco, and P. Bauerfeind, "Is virtual colonoscopy a cost-effective option to screen for colorectal cancer?," *American Journal of Gastroenterology*, vol. 94, no. 8, pp. 2268–74, 1999.

[26] J. B. Pilz, S. Portmann, S. Peter, C. Beglinger, and L. Degen, "Colon capsule endoscopy compared to conventional colonoscopy under routine screening conditions," *BMC Gastroenterology*, vol. 10, p. 66, 2010.

[27] G. Stevension, "Pain following colonoscopy: elimination with carbon dioxide," *Gastrointestinal Endoscopy*, vol. 38, no. 5, pp. 564–7, 1992.

[28] E. S. Dellon, J. S. Hawk, I. S. Grimm, and N. I. Shaheen, "The use of carbon dioxide for insufflation during gi endoscopy: a systematic review," *Gastrointestinal Endoscopy*, vol. 69, no. 4, pp. 843–9, 2009.

[29] R. Y. Fleming, T. B. Dougherty, and B. W. Feig, "The safety of helium for abdominal insufflation," *Surgical Endoscopy*, vol. 11, no. 3, pp. 230–4, 1997.

[30] F. W. Leung, H. S. Aharonian, J. W. Leung, P. H. Guth, and G. Jackson, "Impact of a novel water method on scheduled unsedated colonoscopy in u.s. veterans," *Gastrointestinal Endoscopy*, vol. 69, no. 3, pp. 546 – 50, 2009.

[31] M. Quirini, A. Menciassi, S. Scapellato, P. Dario, F. Rieber, C.-N. Ho, S. Schostek, and M. Schurr, "Feasibility proof of a legged locomotion capsule for the GI tract," *Gastrointestinal Endoscopy*, vol. 67, pp. 1153–8, 2008.

[32] G. Ciuti, P. Valdastri, A. Menciassi, and P. Dario, "Robotic magnetic steering

and locomotion of microsystems for diagnostic and surgical endoluminal procedures," *Robotica*, vol. 28, pp. 199–207, 2010.

[33] D. Burling, S. A. Taylor, S. Halligan, L. Gartner, M. Paliwalla, and C. Peiris, "Automated insufflation of carbon dioxide for mdct colonography: Distension and patient experience compared with manual insufflation," *American Journal of Radiology*, vol. 186, pp. 96–103, 2006.

[34] J. L. Toennies and R. J. Webster III, "A wireless insufflation system for capsular endoscopes," *ASME Journal of Medical Devices*, vol. 3, no. 2, p. 27514, 2009.

[35] G. Ciuti, "Innovative control platforms for robotic micosystems in endoluminal surgery," Master's thesis, Scuola Superiore di Studi Universitari e Perfezionamento Sant' Anna, 2012.

[36] P. Valdastri, R. J. Webster III, C. Quaglia, M. Quirini, A. Menciassi, and P. Dario, "A new mechanism for mesoscale legged locomotion in compliant tubular environments," *IEEE Transactions on Robotics*, vol. 25, pp. 1047–57, 2009.

[37] J. F. Rey, H. Ogata, N. Hosoe, K. Ohtsuka, N. Ogata, K. Ikeda, H. Aihara, I. Pangtay, T. Hibi, S. Kudo, and H. Tajiri, "Feasibility of stomach exploration with a guided capsule endoscope," *Endoscopy*, vol. 42, no. 7, pp. 541–45, 2010.

[38] J. Scheidler, C. Frank, C. Becker, H. Feist, G. Michalski, M. Sch??tzl, A. B??uml, A. Heuck, and M. Reiser, "Virtual colonoscopy using CT and MRI," *Radiologe*, vol. 38, no. 10, pp. 824–31–, 1998.

[39] N. Arber, R. Grinshpon, J. Pfeffer, L. Maor, S. Bar-Meir, and D. Rex, "Proof-of-concept study of the aer-o-scope omnidirectional colonoscopic viewing system in ex vivo and in vivo porcine models," *Endoscopy*, vol. 39, no. 5, pp. 412–17, 2007.

[40] J. K. Patterson, X. G. Lei, and D. D. Miller, "The pig as an experimental model for elucidating the mechanisms governing dietary influence on mineral absorption," *Experimental Biology and Medicine*, vol. 233, pp. 651–64, 2008.

[41] National Digestive Diseases Information Clearinghouse vol. http://digestive.niddk.nih.gov/ddiseases/pubs/colonoscopy/index.aspxNUMBERSYM

[42] A. Seidell, *Solubilities Of Inorganic And Organic Substances*. New York, D. Van Nostrand company, 2nd ed., 1907.

[43] A. E. Schindler, J. A. Schneider, and K. L. Obstein, "Foaming at the mouth: Ingestion of 35% hydrogen peroxide solution," *Clinical Gastroenterol Hepatol*, vol. 10, pp. 13–14, Feb. 2012.

[44] C. T. Dietzel, H. Richert, S. Albert, U. Merkel, M. Hippius, and A. Stallmach, "Magnetic Active Agent Release System (MAARS): Evaluation of a new way for a reproducible, externally controlled drug release into the small intestine," *Journal of Controlled Release*, vol. 161, no. 3, pp. 722–7, 2012.

[45] K. Phaosawasdi, W. Cooley, J. Wheeler, and P. Rice, "Carbon dioxide-insufflated colonoscopy: an ignored superior technique," *Gastrointestinal Endoscopy*, vol. 32, pp. 330–3, 1986.

[46] H. Duthie and J. D. Atwell, "The absorption of water, sodium and potassium in the large intestine with particular reference to the effects of villous papillomas," *Gut*, vol. 4, p. 373, 1963.

[47] J. Sauk and S. Itzkowitz, "Optical enhancements in diagnosis and surveillance of colorectal neoplasia," *Current Colorectal Cancer Reports*, vol. 7, no. 1, pp. 24–32, 2011.